



**UNIVERSIDAD DE INVESTIGACION DE
TECNOLOGÍA EXPERIMENTAL YACHAY**

Escuela de Ciencias Químicas e Ingeniería

**Preparation of Electrochemical Sensors Based on Conducting
Polymers for the Determination of Emergent Pollutants**

Trabajo de integración curricular presentado como requisito para la
obtención del título de Químico

Autor:

Terán Alcocer Álvaro Vinicio

Tutor:

Palma Cando Alex Uriel, PhD

Urququí, septiembre 2020

SECRETARÍA GENERAL
(Vicerrectorado Académico/Cancillería)
ESCUELA DE CIENCIAS QUÍMICAS E INGENIERÍA
CARRERA DE QUÍMICA
ACTA DE DEFENSA No. UITEY-CHE-2020-00054-AD

A los 8 días del mes de octubre de 2020, a las 10:00 horas, de manera virtual mediante videoconferencia, y ante el Tribunal Calificador, integrado por los docentes:

Presidente Tribunal de Defensa	Dr. VILORIA VERA, DARIO ALFREDO , Ph.D.
Miembro No Tutor	Mgs. DE LIMA ELJURI, LOLA MARIA
Tutor	Dr. PALMA CANDO, ALEX URIEL , Ph.D.

El(la) señor(ita) estudiante **TERAN ALCOCER, ALVARO VINICIO**, con cédula de identidad No. **1723153530**, de la **ESCUELA DE CIENCIAS QUÍMICAS E INGENIERÍA**, de la Carrera de **QUÍMICA**, aprobada por el Consejo de Educación Superior (CES), mediante Resolución **RPC-SO-39-No.456-2014**, realiza a través de videoconferencia, la sustentación de su trabajo de titulación denominado: **PREPARATION OF ELECTROCHEMICAL SENSORS BASED ON CONDUCTING POLYMERS FOR THE DETERMINATION OF EMERGENT POLLUTANTS** , previa a la obtención del título de **QUÍMICO/A**.

El citado trabajo de titulación, fue debidamente aprobado por el(los) docente(s):

Tutor	Dr. PALMA CANDO, ALEX URIEL , Ph.D.
--------------	-------------------------------------

Y recibió las observaciones de los otros miembros del Tribunal Calificador, las mismas que han sido incorporadas por el(la) estudiante.

Previamente cumplidos los requisitos legales y reglamentarios, el trabajo de titulación fue sustentado por el(la) estudiante y examinado por los miembros del Tribunal Calificador. Escuchada la sustentación del trabajo de titulación a través de videoconferencia, que integró la exposición de el(la) estudiante sobre el contenido de la misma y las preguntas formuladas por los miembros del Tribunal, se califica la sustentación del trabajo de titulación con las siguientes calificaciones:

Tipo	Docente	Calificación
Tutor	Dr. PALMA CANDO, ALEX URIEL , Ph.D.	10,0
Miembro Tribunal De Defensa	Mgs. DE LIMA ELJURI, LOLA MARIA	10,0
Presidente Tribunal De Defensa	Dr. VILORIA VERA, DARIO ALFREDO , Ph.D.	10,0

Lo que da un promedio de: **10 (Diez punto Cero)**, sobre 10 (diez), equivalente a: **APROBADO**

Para constancia de lo actuado, firman los miembros del Tribunal Calificador, el/la estudiante y el/la secretario ad-hoc.

Certifico que en cumplimiento del Decreto Ejecutivo 1017 de 16 de marzo de 2020, la defensa de trabajo de titulación (o examen de grado modalidad teórico práctica) se realizó vía virtual, por lo que las firmas de los miembros del Tribunal de Defensa de Grado, constan en forma digital.

TERAN ALCOCER, ALVARO VINICIO
Estudiante

Dr. VILORIA VERA, DARIO ALFREDO , Ph.D.
Presidente Tribunal de Defensa

DARIO ALFREDO VILORIA VERA
 Firmado digitalmente por DARIO ALFREDO VILORIA VERA
 Fecha: 2020.10.09 10:58:46 -05'00'

Dr. PALMA CANDO, ALEX URIEL , Ph.D.
Tutor



Firmado electrónicamente por:
ALEX URIEL
PALMA CANDO

Mgs. DE LIMA ELJURI, LOLA MARIA
Miembro No Tutor

LOLA
MARIA DE
LIMA ELJURI

Digitally signed by
LOLA MARIA DE
LIMA ELJURI
Date: 2020.11.04
16:46:54 -05'00'

CIFUENTES TAFUR, EVELYN CAROLINA
Secretario Ad-hoc

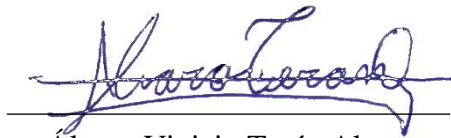


Firmado electrónicamente por:
**EVELYN CAROLINA
CIFUENTES TAFUR**

AUTORÍA

Yo, Álvaro Vinicio Terán Alcocer, con cédula de identidad 1723153530, declaro que las ideas, juicios, valoraciones, interpretaciones, consultas bibliográficas, definiciones y conceptualizaciones expuestas en el presente trabajo, así como, los procedimientos y herramientas utilizadas en la investigación, son de absoluta responsabilidad del autor del trabajo de integración curricular. Así mismo, me acojo a los reglamentos internos de la Universidad de Investigación de Tecnología Experimental Yachay.

Urcuquí, septiembre 2020



Álvaro Vinicio Terán Alcocer

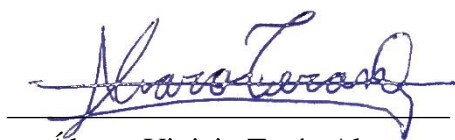
CI: 1723153530

AUTORIZACIÓN DE PUBLICACIÓN

Yo, Álvaro Vinicio Terán Alcocer, con cédula de identidad 1723153530, cedo a la Universidad de Investigación de Tecnología Experimental Yachay, los derechos de publicación de la presente obra, sin que deba haber un reconocimiento económico por este concepto. Declaro además que el texto del presente trabajo de titulación no podrá ser cedido a ninguna empresa editorial para su publicación u otros fines, sin contar previamente con la autorización escrita de la Universidad.

Así mismo, autorizo a la Universidad que realice la digitalización y publicación de este trabajo de integración curricular en el repositorio virtual, de conformidad a lo dispuesto en el Art. 144 de la Ley Orgánica de Educación Superior.

Urcuquí, septiembre 2020



Álvaro Vinicio Terán Alcocer

CI: 1723153530

A mis padres y hermano.

AGRADECIMIENTOS

I would like to thank to:

My dear parents Álvaro and Lucía, and my brother Mateo for their unconditional love and for always been for me.

My beloved Anabel, who has been part of this travel in the university, always giving me help and love.

My friend Pancho with whom I worked in many projects and the thesis itself.

My good friends at Yachay Tech.

My professor and tutor Alex from whom I received teachings that helped me in my academic but also personal training.

The members of the jury, Dr. Alfredo Vilorio, MSc. Lola De Lima and Dr. Alex Palma who helped me improving the quality of this work with revisions and corrections.

Abstract

Chemical waste from different industries and residential areas have become an issue for the environment. Particularly, phenolic compounds, nitrites, pharmaceuticals, nitroaromatic compounds and hydrogen peroxide are hazardous and toxic environmental pollutants released into aquatic ecosystems. Recently, efforts have focused in real-time, quantitative and fast detection methods because commonly used approaches do not fulfill these requirements. In this work, recent progress in conducting polymers (CPs) based electrochemical sensors are reviewed in the last five years, as a promising system for fast, accurate and sensitive detection method for aqueous environmental contaminants. Special focus is put into the preparation and elaboration of the CPs based electrodes for developing microstructures and networks, which can be widely diverse, going from linear structures to tridimensional arrays.

Keywords:

Electrochemical Sensors, conducting polymers, cyclic voltammetry, Differential Pulse Voltammetry, Amperometry, phenolic compounds, nitrites, pharmaceuticals, nitroaromatic compounds, hydrogen peroxide.

Resumen

Los residuos químicos de diferentes industrias y áreas residenciales se han convertido en un problema para el ambiente. En particular, los compuestos fenólicos, nitritos, productos farmacéuticos, compuestos nitroaromáticos y el peróxido de hidrógeno son contaminantes ambientales peligrosos y tóxicos que se liberan a los ecosistemas acuáticos. Recientemente, los esfuerzos se han centrado en métodos de detección rápidos, cuantitativos y en tiempo real porque los enfoques comúnmente utilizados no cumplen con estos requisitos. En este trabajo, los avances recientes en sensores electroquímicos basados en polímeros conductores (CPs) son revisados en los últimos cinco años, como un método prometedor para la detección rápida, precisa y sensible de contaminantes ambientales en medios acuosos. Énfasis especial se ha puesto en la preparación y elaboración de los electrodos basados en CPs para la formación de microestructuras y redes poliméricas, que puede ser muy diversa, pasando de estructuras lineales a matrices tridimensionales.

Palabras Clave:

Sensores Electroquímicos, polímeros conductores, voltamperometría cíclica, Voltamperometría de Pulso Diferencial, Amperometría, compuestos fenólicos, nitritos, farmacéuticos, compuestos nitroaromáticos, peróxido de hidrógeno.

ABBREVIATIONS AND ACRONYMS

CV	Cyclic Voltammetry
DPV	Differential Pulse Voltammetry
DPASV	Differential Pulse Anodic Stripping Voltammetry
CA	Chronoamperometry
SWV	Square Wave Voltammetry
MIP	Molecular Imprinted Polymer
MWCNTs	Multi-walled carbon nanotubes
f-SWCNTs	Functionalized Single-Walled Carbon Nanotubes
AMTEOS	Anilinomethyltriethoxysilane
APTMS	3-aminopropyltriethoxysilane
TEOS	Tetraethyl orthosilicate
CPE	Carbon Paste Electrode
GCE	Glassy Carbon Electrode
GS	Graphene carbon spheres
PGE	Pencil Graphite Electrode
MNZ	Metronidazole
CFX	Ciprofloxacin
ASA	Acetylsalicylic Acid
AuNPs	Gold Nanoparticles
AgNCs	Ag nanocrystals
PTH	Polythionine

FTO	Tin Oxide
PANI	Polyaniline
EBT	Eriochrome Black T
PCC	Poly-catechol
CS	Chitosan
PEB	Poly(Evans Blue)
rGO	Reduced Graphene Oxide
PPR	Poly(Phenol Red)
E2	17- β -Estradiol
HRP	Horseradish Peroxidase
TBA-TFB	Tetrabutylammonium tetra- fluoroborate
γ-PGA	Poly(γ -Glutamic Acid)
ATh	3-Aminothiophene
AA	Acrylic Acid
EGDE	Ethylene Glycol Diglycidyl Ether
SBP	Soybean Seed Coat Peroxidase
poly 2AB	Poly(2-aminophenylbenzimidazole)
PMB	Poly(Methylene Blue)
MPrPt	Mesoporous Platinum
BDD	Boron-Doped Diamond
CQDs	Carbon Quantum Dots
nHAp	Nano-sized Hydroxyapatite
PdNPs	Palladium Nanoparticles
1,5-DAN	1,5-Diaminonaphthalene
CoNS	Cobalt Nanostructures

RC	Resorcinol
HQ	Hydroquinone
CC	Catechol
NG B	Naphthol Green B
TNT	2,4,6-Trinitrotoluene
DNT	2,4-Dinitrotoluene
Tetryl	2,4,6-Trinitrophenylmethylnitramine
PDA	Phenylenediamine
PAR	Poly(Alizarin Red)
p-ABSA	p-Aminobenzene Sulfonic Acid
PME	Poly(Melamine)
NFT	Nitrofurantoin
NFZ	Nitrofurazone
FTD	Furaltadone
FZD	Furazolidone
NP	Nitrophenol
35DT	3,5-Diamino-1,2,4-Triazole
SDS	Sodium Dodecyl Sulphate
PPy	Poly(Pyrrole)
ENPPy	Nano Poly(Pyrrole)
PPy3C	Poly(Pyrrole-3-Carboxylic Acid)
PEDOT-SH	Poly(Thiomethyl 3,4-Ethylenedioxythiophene)
PEDOTM	Poly(Hydroxymethylated-3,4-Ethylenedioxythiophene)
PEDOT:PSS	Poly(3,4-Ethylenedioxythiophene) Polystyrene Sulfonate
Pol	4,7-bis(5-(3,4- Ethylenedioxythiophene)thiophen-2-yl)Benzothiadiazole

Index

CHAPTER I: General Introduction.....	1
1.1 Introduction	1
1.2 Problem Statement	7
1.3 Objectives.....	8
1.3.1 General Objective	8
1.3.2 Specific Objectives	8
CHAPTER II: State-of-the-Art Review	9
2.1 Diverse Pharmaceuticals	9
2.1.1 Metronidazole (MNZ).....	9
2.1.2 Acetylsalicylic acid (ASA)	11
2.1.3 9-carboxymethoxymethyl guanine (Acyclovir).....	11
2.1.4 Ciprofloxacin (CFX).....	13
2.1.5 17- β -Estradiol (E2)	14
2.1.6 Paracetamol (PR)	15
2.2 Hydrogen peroxide.....	22
2.2.1 Enzymatic Detection.....	22
2.2.2 Enzymeless Detection.....	23
2.3 Nitrites.....	26
2.4 Phenolic Compounds.....	30
2.5 Nitroaromatic Compounds	34
Conclusions and Recommendations	39
Conclusions.....	39
Recommendations	40
References	41

CHAPTER I: General Introduction

1.1 Introduction

Environmental pollutants have become an issue of great importance during recent decades¹. These compounds resulting from agricultural, paints, textile, plastic, pharmaceutical, petroleum and other industries, are widely released into aquatic ecosystems². Among all of these pollutants, phenolic compounds, nitrites, pharmaceuticals, nitroaromatic compounds and hydrogen peroxide are very hazardous, because of its high toxicity, carcinogenicity and low biodegradability³, producing skin damage, necrosis, methemoglobinemia, drowsiness, nausea and many others⁴⁻⁶.

Real-time, quantitative and fast detection methods are required⁷. However, commonly used methods such as gas chromatography, mass spectrometry⁸, and high-performance liquid chromatography⁹ are time-consuming and expensive, as well skilled operators and pretreated samples are usually required¹⁰. On the other hand, polymeric biosensors have the advantage of being simple, with direct transduction, high selectivity, high sensitivity, miniaturization, ease of use, and low cost^{11,12}. Thus, opening a new approach for research and development of electrodes.

A chemical sensor is a device composed by a recognition element (receptor) coupled with a physico-chemical transducer, which transforms chemical information into analytical signals^{13,14}. When the recognition system utilizes a biochemical mechanism is categorized as biosensor¹⁵. These sensors are classified depending on the property that will be analyzed. Thus, electrical, optical, mass, thermal, among other sensors can be found¹⁶. Electrochemical sensors and biosensors, having an electrochemical transducer, convert chemical energy into electrical energy, when a chemical reaction takes place on the working electrode¹³. The solution where the reaction occurs can be in gaseous, liquid or solid state¹⁷. Compared to others, electrochemical sensors are especially attractive because of their remarkable detectability, experimental simplicity and low cost¹⁸. There are four main types of electrochemical sensors: potentiometric, conductometric, voltammetric and amperometric¹⁹. The scope of this investigation will cover the last two types.

The electrochemical sensors have evolved through the employment of novel modifier materials, such as conductive polymers and carbon nanomaterials^{20,21}, because the immobilization transfers the physicochemical properties of the modifier to the electrode surface, showing high surface area, excellent thermal conductivity²², electric conductivity³ and strong mechanical strength^{19,23,24}. Most polymers are applied to electrode surfaces by a combination of adsorptive attraction and low solubility in the electrolyte solution, using pre-formed polymers or electrochemical polymerization²⁵. Electronically conducting polymers such as poly(pyrrole) or poly(thiophene), have attracted considerable attention due to their good film-forming property, high electrical conductivity, high transparency in the visible region, and excellent thermal and environmental stability²⁶. Different types of nanoparticles can be doped together with the polymers forming composites²⁷, allowing the combination of the properties which can improve the mechanical, optical, and electrical properties of polymer without sacrificing its processability or adding excessive weight²⁸.

1.1.1 Voltammetric sensors

In these sensors, the solutes in the solution interact at the surface of the electrode, where the potential can be controlled, undergoing oxidation or reduction which produces the current that is measured²⁹. In voltammetric measurements the current measured consists of two components: faradaic current and non-faradaic or charging current. The faradaic current originates from electrochemical reactions and is proportional to the concentration of the analyte³⁰. The charging current, however, is not an analytical signal, it is formed when the double layer at the working electrode is charged or discharged when the potential of the electrode is changed¹⁶. Different voltammetric techniques have been used in order to eliminate the charging current and enhancing the faradaic current, from all of them, the most used for organic molecules sensing are cyclic voltammetry, differential pulse voltammetry and amperometry.

1.1.1.1 Cyclic Voltammetry

Cyclic Voltammetry (CV) consists on applying different potentials to the working electrode, making a scan, until a certain potential in which the scanning is reversed³¹. The potential of

this working electrode is controlled versus a reference electrode³². The applied signal for CV is a triangular waveform (Figure 1a), where the scan rate is observed as the slope of the curve.

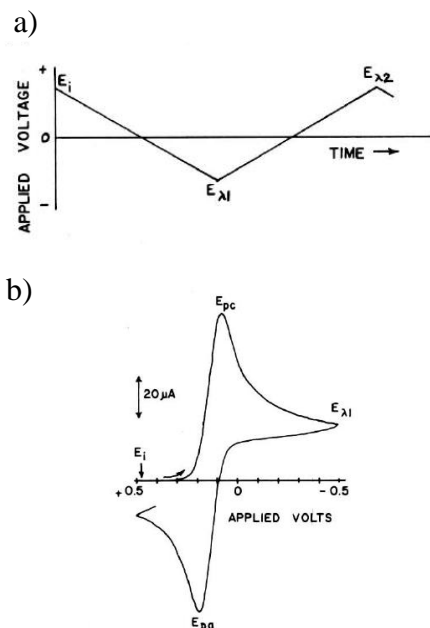


Figure 1. a) Applied potential program for a complete cycle. b) Typical cyclic voltammogram for reversible electroactive species. Modified with permission from [32]. Copyright 1983 American Chemical Society.

The voltammogram is obtained by measuring the response signal versus the potential (Figure 1b). This signal is the current at the working electrode during the potential scan³³. The important parameters are the magnitudes of the anodic, cathodic, peak currents and peak potentials³⁴. The peak current for a reversible system is described by the Randles-Seveik equation:

$$i_p = (2.69 \times 10^5) n^{3/2} A D^{1/2} C v^{1/2} \quad (1)$$

where i_p is peak current, n are the electrons exchanged in the reaction, A is the electroactive area (cm^2), D is diffusion coefficient (cm^2/s), C is concentration (mol/cm^3), and v is scan rate (V/s). The relationship to concentration is particularly important in analytical applications and in studies of electrode mechanisms. However, the ratio of peak currents can be significantly influenced by chemical reactions coupled to the electrode process³⁵.

1.1.1.2 Differential Pulse Voltammetry

Differential pulse voltammetry (DPV) enhances discrimination of faradaic current from non-faradaic current. In this technique amplitude potential pulses are applied upon a staircase waveform ramp potential³⁶. A base potential value is chosen and then the scan starts, the potential increases between pulses with equal increments. The current is immediately measured before the pulse application and at the end of the pulse, and the difference between them is recorded³⁷ (Figure 2a).

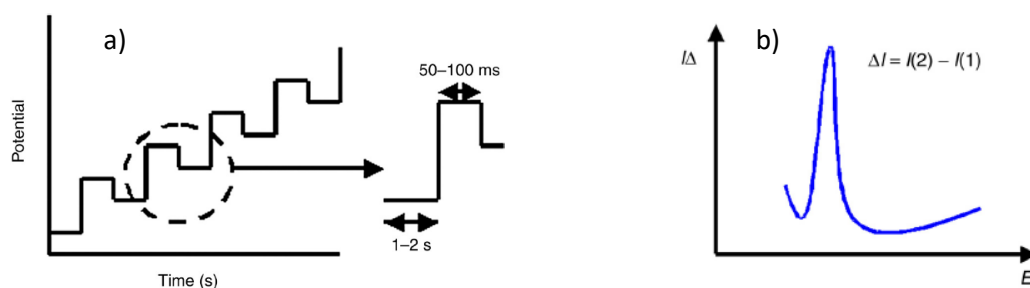


Figure 2. a) Diagram of the application of pulses in the differential pulse voltammetry (DPV) technique. b) Typical response of a differential pulse voltammogram. Modified with permission from [37]. Copyright 2017 Elsevier.

The difference of currents against the potential produces the DPV voltammogram (Figure 2b). DPV is more sensitive than linear sweep methods because there is a minimization of the capacitive current^{38,39}. Therefore, CV is commonly used for exploratory purposes and DPV for quantitative determinations^{40,41}.

1.1.2 Amperometric sensors

In Amperometric sensors a constant potential is applied between a reference and a working electrode⁴². When the constant potential is applied, the electroactive species are oxidized or reduced at the electrode surface and is observed as a variation in current which is recorded^{40,43}. The obtained current is directly related to the bulk concentration of the electroactive species¹³, as is observed in Figure 3, in which a sensor made of Pyrrole, 1-(2-Carboxyethyl)pyrrole and Alcohol Dehydrogenase was used for Ethanol determination⁴⁴.

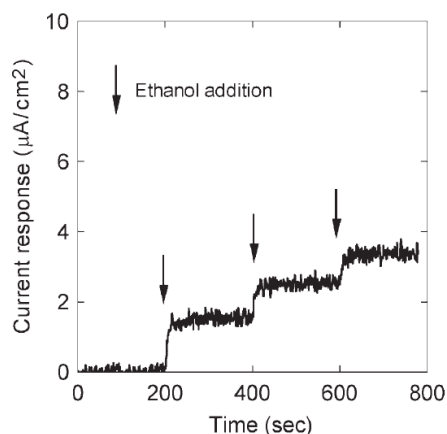


Figure 3. Typical amperometric response to ethanol with a sensor doped with Pyrrole and 1-(2-Carboxyethyl)pyrrole. Reproduced with permission from [44]. Copyright 2010 John Wiley and Sons Inc.

Amperometric sensors display high sensitivity, wide detection range, short response time and the ability to distinguish selectively between a number of electroactive species in solutions¹⁹. According to the Cottrell equation, the resulting current can be related to the concentration of the electroactive species as follows:

$$I = \frac{n F A D^{1/2} C_b}{\pi t} \quad (2)$$

where I corresponds to the diffusion current (mA), t electrolysis time (s), n is the number of electrons involved in the reaction, A is the electrode area (m^2), D is the diffusion coefficient ($m^2 s^{-1}$), F is the Faraday constant and C_b is the bulk concentration of the electroactive species ($mmol L^{-1}$). This kind of sensors are based on a technique known as *chronoamperometry*⁴⁵, where current is plotted against time. The main requirements in chronoamperometry are (i) the transport of the electroactive species must be governed by diffusion, and (ii) the electrode surface must remain constant^{38,46}.

1.1.3 Instrumental analysis

Instrumental methods can perform analyses that are difficult or impossible by classical methods⁴⁷. Classical concentration analysis ranges 2–3 orders of magnitude, while instrumental tools such electrochemical methods are capable of sensing over a range of six or more orders of magnitude reaching trace and ultra-trace quantities of analytes⁴⁸. The advantage of this methods is that are able to be combined with statistical procedures providing useful

information of the measurements. Focused on electrochemical sensors, calibration curves and limits of detection will be covered.

1.1.3.1 Calibration graphs

For the elaboration of the graphs, several analytes with different known concentrations are required⁴⁹. These calibration standards are measured with the analytical instrument under the same conditions, in this case a potentiostat, with SWV as measuring method (Figure 4). The current measurements are plotted against the concentrations⁵⁰.

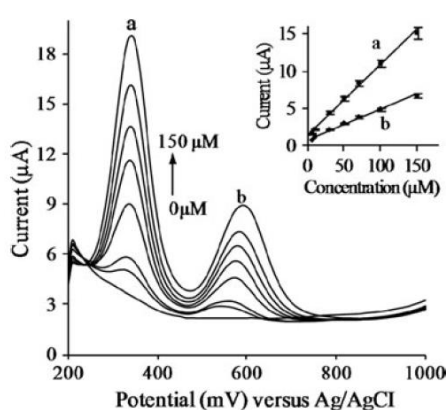


Figure 4. Square wave voltammograms for different concentrations of paracetamol and p-aminophenol. Inset: calibration plots for both analytes. Reproduced with permission from [51]. Copyright 2015 Taylor and Francis Ltd.

The statistical analysis can be performed to the linear portion of the graph. In this segment, unknown samples can be determined by interpolation due to regression equations⁵¹. It is crucial to include the 'blank' in the calibration curve, because specially in electrochemical measurements the signal given by the blank is not zero and contains the information of solvent and reagents without taking into account the electroactive species⁵².

1.1.3.2 Limit of detection

Environmental pollutant substances are found in trace concentrations, which require methods with low limits of detection⁵³. It is understood as limit of detection of an analyte to the concentration which gives a signal *significantly different* from the 'blank'⁵⁴. An analytical

definition implies that the limit of detection (LOD) is equal to the standard deviation (σ) of the blank multiplied by 3 and divided by the slope of the curve (M)⁵⁵.

$$LOD = \frac{3\sigma}{M} \quad (3)$$

1.2 Problem Statement

Emerging contaminants are chemicals with potential health effects associated with human exposure that have been widely distributed in the environment⁵⁶. These compounds can be found in aqueous environments dispersing and persisting to a great extent⁵⁷. Many contaminants are difficult to remove in conventional wastewater treatment systems, so these facilities are another source of emerging pollutants⁵⁸. A large number of contaminants such pharmaceuticals, phenolic compounds, nitrites, nitroaromatic compounds and hydrogen peroxide have been found in surface waters. Phenols are derived from industrial wastewater⁵⁹, used in the production of aromatic compounds such explosives, fertilizers, paint, paint removers, textile, plastics and drugs^{60,61}. Exposures to phenolic compounds damage to the lungs, liver, kidneys and genito-urinary tract⁶². Nitrites are found as well in food and physiological systems⁶³, producing carcinogenic nitrosamines⁶⁴. As fertilizer, it can highly impact water sources⁶⁵. Nitroaromatics are the major components of explosives and used, residues can accumulate in the environment⁶⁶. Many tools have been used for the determination of these compounds such spectroscopic and chromatographic methods⁶⁷. However, they are laborious and time-consuming procedures⁶⁸. For that reason, electrochemical detection has been developed, overcoming the difficulties of normally used techniques^{69,70}. Moreover, multiple efforts are oriented to the development of electrochemical sensors due to its potential. Some of these sensor devices have reached commercialization and routinely usage⁷¹. This investigation is focused on generating a state-of-the-art review of studies about the advances and approaches for sensing and determining emerging contaminants using CPs based electrochemical sensors.

1.3 Objectives

1.3.1 General Objective

- ◆ To analyze the recent progress in the conducting polymers based electrochemical sensors for determination of various emergent contaminants.

1.3.2 Specific Objectives

- ◆ To investigate the preparation methods of the conducting polymers based electrochemical sensors.
- ◆ To interpret the microstructure in terms of function of the polymeric nanostructures.
- ◆ To determine the relationship between the polymeric nanocomposites and the response of the electrochemical sensors for the determination of phenolic compounds, nitrites, pharmaceuticals, nitroaromatic compounds and hydrogen peroxide.

CHAPTER II: State-of-the-Art Review

2.1 Diverse Pharmaceuticals

2.1.1 Metronidazole (MNZ)

MNZ is a nitro-compound used for treating diseases caused by protozoa or anaerobic bacteria⁷². This nitro-compound was sensed with a duplex molecularly imprinted polymer (DMIP) hybrid film composed of **poly(anilinomethyltriethoxysilane)** (poly(AMTEOS)) and an imprinted polysiloxane layer on a carbon paste electrode (DMIP/CPE)⁷³. Figure 5 shows a schematic preparation of DMIP/CPE for sensing of MNZ. Poly(AMTEOS) was electrogenerated at the carbon paste electrode (CPE) by cyclic voltammetry. Then, a solution containing 3-aminopropyltriethoxysilane (APTMS), tetraethyl orthosilicate (TEOS), 2-ethoxyethanol and MNZ, was drop casted onto the modified electrode, where triethoxysilyl groups were hydrolyzed forming a MIPS film over the conductive polyaniline layer. DMIP/CPE exhibited a rough surface, because of the formation of imprinted cavities, which increased the surface area. Electrocatalytic activity and recognition were enhanced due to (i) the amino group from APTMS that forms hydrogen bonds with the oxygen or nitrogen atom in MNZ, and (ii) the phenyl units of the conductive polymer which presented “ π - π stacking” interaction with the aromatic heterocycle of MNZ. Under optimized conditions, the reduction peak currents were linearly proportional to the MNZ concentrations in the range from 0.4 μ M to 0.2 mM with a detection limit of 91 nM by using a DPV sensor.

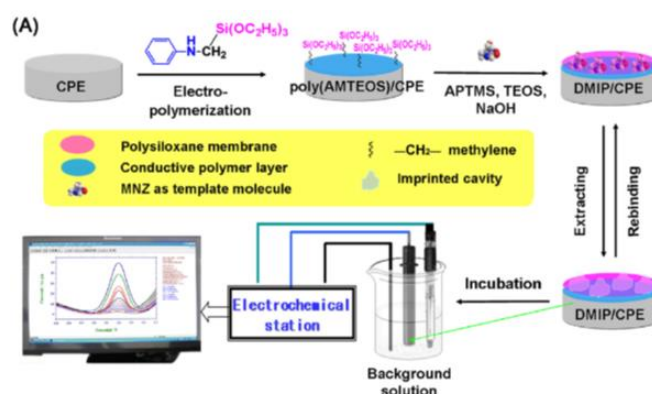


Figure 5. Schematic illustration for the preparation of DMIP/CPE. Modified with permission from [73]. Copyright 2016 Elsevier.

An electrode based on molecularly imprinted polymer with gold nanoparticles sensed MNZ with a detection limit of 0.12 μM . A suspension of AuNPs and chitosan was dropped on the surface of the GCE. The modified AuNPs/GCE was immersed in an aqueous solution containing CuSO_4 , H_2SO_4 , NaCl , metronidazole and melamine, where electrodeposition was carried by cyclic voltammetry. The template (metronidazole) was extracted in Britton–Robinson buffer with multiple cycles. The MIP/AuNPs/GCE has a smooth surface, where the polymeric layers show folded structure (Figure 6a). When the template is removed, a rougher layer is observed (Figure 6b). The catalytic activity can be associated to the mimetic enzyme center formed by the copper ions, which facilitates the conduction of electrons. The polymeric film emulates the microenvironment for the enzymatic reaction, which is better catalyzed in the large surface area of the polymer. Using DPV, the response to metronidazole was linear in the concentration range of 0.5 μM to 1000 μM ⁷⁴.

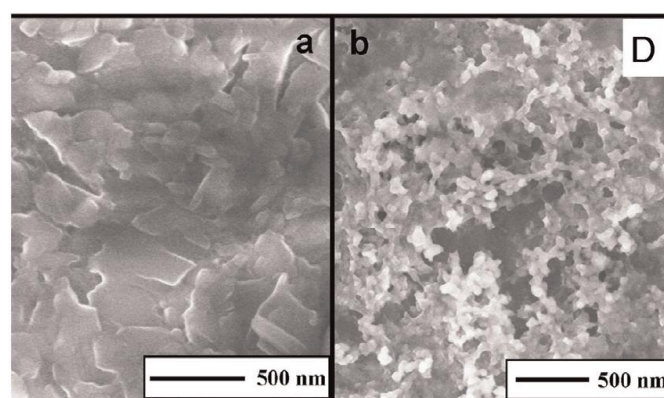


Figure 6. MIP/AuNPs/GCE microstructure before (a) and after (b) metronidazole extraction. Modified with permission from [74]. Copyright 2015 Elsevier.

Similarly, MNZ was determined with a three-dimensional graphene-like carbon architecture (3D-HPG) and polythionine (PTH) modified glassy carbon electrode (GCE)⁷⁵. The PTH-modified GCE was prepared by cyclic voltammetry in H_2SO_4 solution containing thionine. The 3D-HPG suspension was casted in the surface of the modified electrode and dried under infrared lamp. The PTH film was uniform through all the surface. But, after the drop-casting, a continuous 3D porous network with macropores can be observed. The PTH film increases the electrical conductivity and the 3D-HPG accelerates the electron transfer rate due to its large high surface area, greatly improving the electrochemical sensing. Two linear ranges were

observed with DPV, from 0.05 μM to 70 μM and 70 μM to 500 μM with a detection limit of 1 nM.

2.1.2 Acetylsalicylic acid (ASA)

Asa is an important nonsteroidal anti-inflammatory⁷⁶, analgesic⁷⁷ and antipyretic drug⁷⁸. However, is also known to have effects such as gastric acid secretion and dieresis if abused. A new electrochemical sensor made of manganese dioxide (MnO_2)- antimony trioxide (Sb_2O_3) together with polyaniline (PANI) on tin oxide (FTO) electrode ($\text{MnO}_2\text{-Sb}_2\text{O}_3/\text{PANI}/\text{FTO}$) was used for sensing ASA in urine. The modified electrode was prepared in HCL by cyclic voltammetry in two steps. First containing aniline, and then replacing it with $\text{Mn}(\text{NO}_3)_2$ and SbCl_3 . The PANI film showed large lumpy shapes and clews structures. When, $\text{MnO}_2\text{-Sb}_2\text{O}_3$ was deposited, the composite agglomerated into a globular structure. Improvement in electron transfer kinetics was attributed to large surface area and high electrocatalytic activity of PANI as well as providing high current density, specific surface area and thermal conductivity. MnO_2 and Sb_2O_3 increased the catalytic activity and stability of PANI, enhancing electrochemical detection performance. Under optimal conditions with DPV, the $\text{MnO}_2\text{-Sb}_2\text{O}_3/\text{PANI}/\text{FTO}$ electrode showed a linear range of 1.2 nM to 228.68 nM with detection limit of 0.20 nM⁷⁹.

A novel electrochemical imprinted sensor based on polypyrrole, sol-gel and $\text{SiO}_2@\text{Au}$ core-shell nanoparticles showed linear response to ASA concentration using square wave voltammetry. The range went from 1.0 nM to 10.0 nM and 10.0 nM to 100.0 nM with a limit of detection of 0.2 nM. The deposition on Au electrode was carried out by one step using cyclic voltammetry in a solution containing phenyltriethoxysilane, tetraethoxysilane, ethanol, trifluoroacetic acid, ASA, lithium perchlorate, pyrrole and $\text{SiO}_2@\text{AuNPs}$. The silane monomers were used to prepare the imprinted sol-gel film, TEOS as the cross-linker and PTEOS as the functional monomer for $\pi\text{-}\pi$ interactions with aromatic ring. Pyrrole increased the stability of the resultant MIP and enhancing the conductivity⁸⁰.

2.1.3 9-carboxymethoxymethyl guanine (Acyclovir)

Acyclovir is used as antiviral drug⁸¹ for the treatment of herpes simplex and zoster infections⁸². A sensitive sensor made of Eriochrome black T deposited on a glassy carbon electrode

(PEBT/GCE) was used for detecting Acyclovir by DPV. The PEBT film was electrodeposited on GCE surface with cyclic voltammetry in NaOH solution. After deposition, uniform branch-like structures covered all the active area, enlarging the effective electrode surface in approximately 2.4 times. The polymeric film increased the electrocatalytic activity and electrical conductivity. The peak current was linearly related with Acyclovir concentration in acetate buffer, from 0.03 μM to 0.3 μM and 0.3 μM to 1.5 μM , with a detection limit of 12 nM⁸³.

Using multi-walled carbon nanotubes (MWCNTs) and TiO₂ nanoparticles (TiO₂ NPs) together with poly-catechol (PCC) as polymeric matrix in a nanoporous glassy carbon electrode, a new sensor was developed for Acyclovir determination⁸⁴. The catechol was electrodeposited on nanoporous GCE by cyclic voltammetry in a PBS buffer. An acetic acid solution containing TiO₂ NPs, MWCNTs and chitosan (CS) was dispersed on the modified electrode. The nanoporous GCE (Figure 7b) showed a rougher surface compared to standard GCE (Figure 7a), which increased when PCC was deposited (Figure 7c), showing high porosity. After drop-casting, the irregularity of the surface increased highly, showing randomly tangled spaghetti-like carbon nanotubes, as well as granular morphology by TiO₂ NPs (Figure 7d).

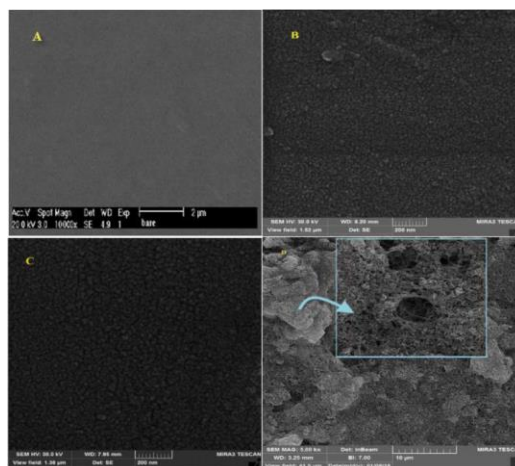


Figure 7. FESEM images of: (A) Bare GCE, (B) nanoporous GCE, (C) PCC/ nanoporous GCE and (D) CS-MWCNTs+TiO₂ NPs/ PCC/ nanoporous GCE. Reproduced with permission from [84]. Copyright 2018 Electrochemical Society, Inc.

The polymeric film improved the catalytic activity toward the ACV oxidation due to its higher surface area and conductivity. Furthermore, when CS-MWCNTs+TiO₂ NPs was drop-casted, the peak current increased highly, showing that the simultaneous presence of nanoparticles and polymer facilitates the electron transfer kinetic and increases the sensitivity of the electrode. The response of the electrode to the Acyclovir concentration using DPASV was linear from 0.03 μM to 1.0 μM with a detection limit of 0.01 μM .

2.1.4 Ciprofloxacin (CFX)

CFX is used in the treatment of numerous bacterial diseases such as pulmonary, respiratory⁸⁵, skin, urinary, ocular, and digestive infections⁸⁶. A novel sensor based on Anionic Surfactant and Polymer Modified on Carbon Paste Electrode has been developed for sensing CFX. Evans blue monomer was electrodeposited by cyclic voltammetry on CPE. Later, SDS was immobilized on the surface, obtaining the SDS/PEB/CPE. The surface of the carbon paste electrode contains irregular flake structures from the graphite paste (Figure 8a). When the polymeric film is added, the surface turns more uniform and regular (Figure 8b). Whereas at the SDS/PEB/CPE surface, the absorbed surfactant molecules show spherical shapes, distributed through all the surface (Figure 8c). The synergetic effect of poly(evans blue) and SDS catalyzes the reaction, where poly(evans blue) increases the conductivity as well as the surface area and the surfactant allows a greater adsorption of CFX which accelerates the rate of electron transfer. The linear response of the SDS/PEB/CPE to CFX concentration ranges from 2 μM to 45 μM and 50 μM to 90 μM with a detection limit of 0.183 μM ⁸⁷.

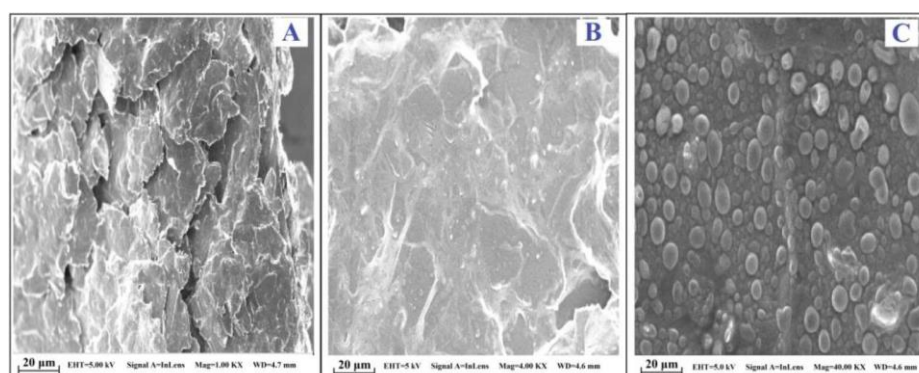


Figure 8. FE-SEM micrographs of A) CPE B) PEB/CPE and C) SDS/PEB/CPE. Reproduced with permission from [87]. Copyright 2019 Wiley-Blackwell Publishing Ltd

CFX was determined with a highly selective electrode based on reduced graphene oxide and poly-phenol red (PPR)⁸⁸. Phenol red was electropolymerized by cyclic voltammetry on the surface of a GCE in PBS. Graphene oxide (GO) was reduced with hydrazine hydrate and dissolved in water. The rGO was drop-casted on the PPR/GCE surface and dried under IR lamp. The microstructure of PPR revealed a sponge sheet-like structure with certain corrugations. After the drop-casting, rGO showed a wrinkled surface morphology. The rGO/PPR composite exhibited both characteristics, in which the spongy sheet-like structures was covered by wrinkled rGO nanosheets. PPR film exhibited high catalytic activity and rGO enhanced the sensitivity. The defects observed in the rGO/PPR film increased the total surface area because of the electrostatic interactions between unoxidized oxygen atoms and the conducting polymer. Under optimal conditions, current response showed a linear relationship with CFX concentration in the ranges from 0.002 μM to 0.05 μM and 0.05 μM to 400 μM , with a low detection limit of 2 nM.

2.1.5 17- β -Estradiol (E2)

E2 and other naturally and man-made chemicals are able to mimic endogenous hormones⁸⁹. They can interfere with the proper functioning of hormonal, immune and nervous systems of mammals⁹⁰. Zhang et al. fabricated a polymeric/enzymatic biosensor for sensing E2 with 4,7-bis(5-(3,4- ethylenedioxythiophene)thiophen-2-yl)benzothiadiazole (Pol) and horseradish peroxidase (HRP) on a platinum electrode. The monomer was dissolved in dichloromethane solution containing tetrabutylammonium tetra- fluoroborate (TBA-TFB) and electrodeposited in the surface of the Pt electrode with chronoamperometry. Afterwards, the HRP was immobilized on the surface of the Pol/Pt electrode using glutaraldehyde as covalent cross-linker. The Pol/Pt surface showed uniformly distributed granular structures. The formed pores allowed the enzyme to anchor and maintain its catalytic activity. The polymer improved the reaction in two ways. First, acting as electron mediator increasing the electron transfer between the enzyme's active center and the electrode surface. Second, creating an appropriate microenvironment to immobilize the protein. The response of HRP/Pol/Pt electrode to 17 β -estradiol concentration was effective in the range from 0.1 μM to 200 μM with a detection limit of 105 nM⁹¹.

The poly(3,6-diamino-9-ethylcarbazole) based molecularly imprinted polymer electrode developed by Liu et al⁹². showed to be an ultra-sensitive and selective sensor for detecting 17- β -estradiol even at attomolar (aM) concentrations. The electrodeposition of the monomer (3, 6-diamino-9-ethylcarbazole) was carried out by cyclic voltammetry in a mixed solvent solution of ethanol and acetate buffer containing the template (17- β -estradiol). Then, the removal of the template was made by washing in a stirring solution of H₂SO₄/ethanol. The surface was observed to be rough with micro islands of poly(3, 6-diamino-9-ethylcarbazole). These islands worked as active sites for the recognition of 17- β -estradiol. Liu et al. found a linear relationship between the Rct value of the EIS response and the logarithm of 17- β -estradiol concentrations (Figure 9). The quantification of 17- β -estradiol showed a wide linear range from 1 aM to 10 μ M with a very low detection limit of 0.36 aM.

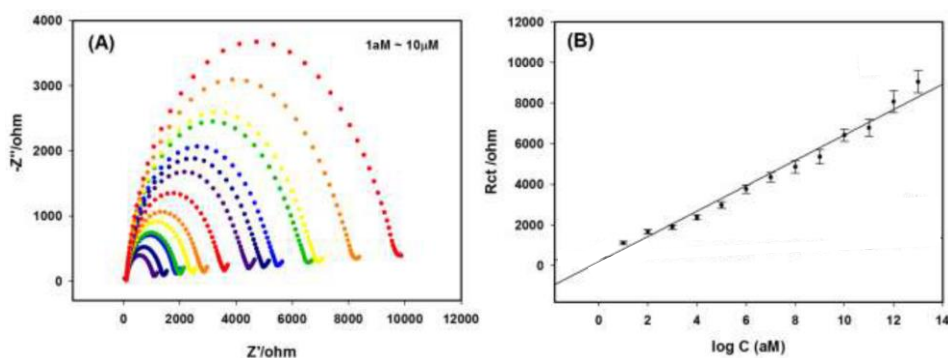


Figure 9. (A) EIS response of the MIP sensor towards 17- β -estradiol in the concentration of 1aM to10 μ M. (B) Calibration curve of the Rct values versus the logarithm concentration of 17- β -estradiol. Modified with permission from [92]. Copyright 2018 Elsevier.

2.1.6 Paracetamol (PR)

PR is a, rapidly metabolized, analgesic and antipyretic drug⁹³. Normally, is a safe analgesic agent, but excessive and long-term usage may lead to the accumulation of toxic metabolites, which leads to liver and kidney damage⁹⁴. A glassy carbon electrode modified with Prussian Blue (PB) and a molecularly imprinted polypyrrole was developed for the sensitive determination of PR⁹⁵. PB film was electrodeposited and activated by cyclic voltammetry in a HCl solution containing FeCl₃·6H₂O, K₃[Fe(CN)₆], and KCl. The activation of the film was carried out in the same solution without the iron species. PB/GCE was immersed in a solution

with pyrrole and PR. Using CV, the polymer was deposited in the surface of the electrode and changing the solution to PBS containing KCl, PR was extracted. PB film showed irregularly shaped crystals suited in nanoclusters. After the electropolymerization of polypyrrole, the surface became smoother, but the porosity increased. DPV was used for sensing the peak current of PR but also for PB signal since Dai et al. used a ratiometric strategy. Using DPV measurements, it was found that addition of PR not only increased the peak current of PR oxidation, but decreased the current for PB signal due to partial blocking of the channels which results in reduced electron transmissivity. The ratio between the mentioned currents and the PR concentration was found to be linear in the range of 1.0 nM to 0.1 mM with a low detection limit of 0.53 nM.

Li et al. fabricated a Poly(3-Methylthiophene) (P3MT)/Reduced Graphene Oxide (rGO) Modified Glassy Carbon Electrode for sensing PR. Graphene oxide (GO) was reduced with hydrazine hydrate and added to DMF. The suspension was drop-casted in a polished GCE and dried under N₂ atmosphere. The P3MT electrodeposition by CV in acetonitrile solution containing methylthiophene and LiClO₄. P3MT/RGO/GCE displays a rough wrinkled surface indicating that RGO was dispersed uniformly and a homogeneous deposition of P3MT. Without the RGO, the reaction is irreversible with only the anodic peak well defined. P3MT/RGO/ GCE not only increases reversibility of the redox reaction, but enhances the response, which is prove of a remarkable synergistic effect. Under optimal conditions, using DPV, the anodic peak current varies linearly with PR concentration in the range of 0.2 μM to 2.5 μM with a limit of detection of 0.025 μM⁹⁶.

A Poly Luminol/Functionalized Multi-Walled Carbon Nanotubes Modified Glassy Carbon Electrode was developed as a highly sensitive sensor for PR detection⁹⁷. f-MWCNTs were dispersed in dimethylformamide (DMF) and casted on the surface of the GCE. Luminol was electrodeposited in H₂SO₄ solution by CV. The bare GC electrode (Figure 10a) showed uniform non-porous surface, while f-MWCNTs/GCE displayed tube-shaped structure from the nanotubes (Figure 10b). After luminol electropolymerization, the diameters of the MWCNTs were larger, with more agglomeration (Figure 10c). The polymer film (PLum) contains a distribution of reduced and oxidized regions. PR accumulates in the reduced regions because of the higher hydrophobic nature. Thus, the anodic peak of PCM shows better response. Using

SWASV in BR buffer solution (pH 7.0), The electrode showed two linear responses (Figure 10d) in the range of 0.04 μM to 32.2 μM and 32.2 μM to 172.2 μM with a limit of detection of 0.025 μM .

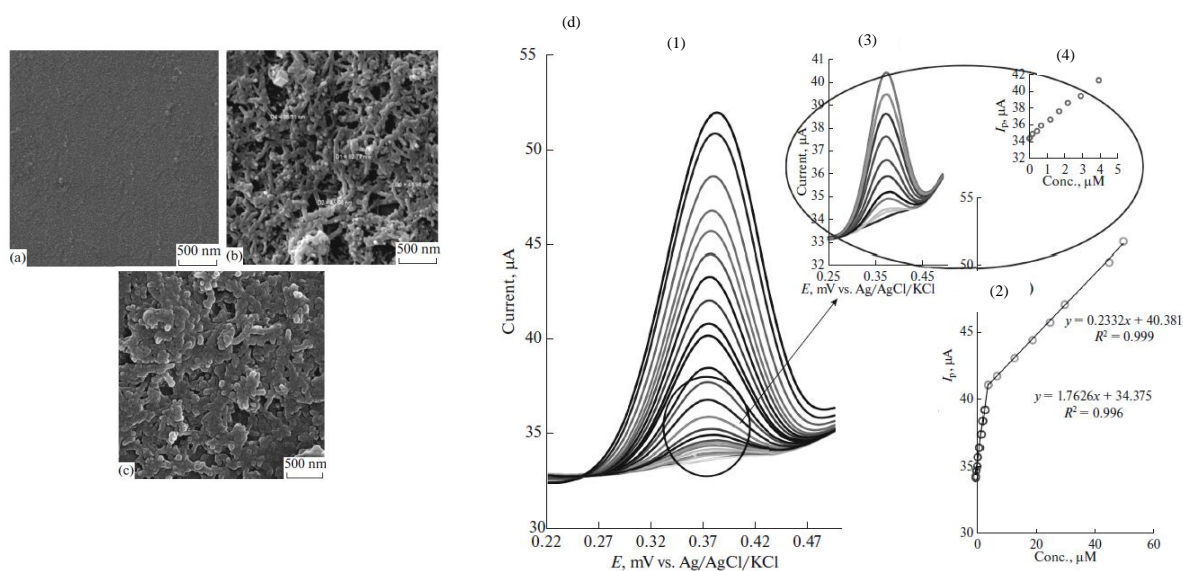


Figure 10. Micrographs of a) bare GCE, b) f-MWCTs/GCE, c) PLum/f-MWCNTs/GCE, d) (1) SWASV responses and (2) calibration curves in two linear ranges. (3) and (4) refers to very low concentrations of PR. Modified with permission from [97]. Copyright 2019 Springer.

Electrodes based on poly(3,4-ethylenedioxythiophene) (PEDOT), with and without multi-walled carbon nanotubes (MWCNT) were developed for PR sensing⁹⁸. In both sensors, the deposition was carried out by potentiostatic electrolysis in a solution containing EDOT and poly(4-lithium styrenesulfonic acid) (PSSLi), the difference was only the presence of (MWCNT) in one of them. The PEDOT:PSSLi/GCE showed a rough surface and high grain composition. PEDOT:PSSLi:MWCNT display a rougher, uniform, dense and compact layer on the surface of the GCE. Carbon nanotubes are observed as tubular-shape structures which increase the surface area. PEDOT film acts as conductive phase and redox mediator, whereas PSSLi dopes with its anion groups the oxidized form of PEDOT improving the mechanical properties of the composite. Using DPV, PEDOT:PSSLi/GCE is capable of sensing PR, but there is no signal if adsorptive stripping differential pulse voltammetry (AdSDPV) is used. However, PEDOT:PSSLi:MWCNT/GCE gives a better response with AdSDPV because carbon nanotubes enable the adsorption paracetamol. Using DPV, PEDOT:PSSLi/GCE displayed a linear response to PR concentration from 0.14 μM to 400 μM . While

PEDOT:PSSLi:MWCNT/GCE with AdSDPV showed linear response in the range from 1.5 μM to 500 μM . The limits of detection were 0.05 μM and 0.08 μM , respectively.

PR was detected by a novel microbial biosensor based on PANI / multiwalled carbon nanotubes⁹⁹. MWCNTs were dispersed in piranha solution. The suspension was added to a solution containing aniline, HCl and KCl and a gold electrode was immersed. Electrodeposition was carried out by CV, obtaining the MWCNT/PANI/ Au electrode. Lyophilized *Bacillus* sp. cells were dissolved in PBS (pH 7.0) and dip-coated onto the modified electrode. After dried, the modified electrode was immersed in glutaraldehyde solution. EIS revealed that bare Au electrode has a small semicircle, but with PANI-cMWCNT, the electron transfer resistance increases significantly. However, in CV analysis, when paracetamol is added, the anodic peak current increases dramatically, due to the enzymatic reduction reaction. The composite enhanced the sensitivity of Au electrode and π - π stacking interactions between MWCNT and PANI provided good stability and conductivity. Amperometric responses showed linearity between 5 μM to 630 μM with a detection limit of 2.9 μM .

A voltammetric study of PR was developed using a poly (rhodamine B) - modified carbon paste electrode (CPE). The monomer rhodamine B was electropolymerized by CV in a NaOH solution. CPE showed the normal irregularly flakes shaped structure. After the polymerization, the film had a uniform arrangement covering the flakes, which increases the surface area. Poly (rhodamine B) accelerates the electrochemical reaction and reduces the overpotential which improves the oxidation current signal. The modified electrode showed good selectivity and sensitivity with a CV linear response for PR concentration ranging 20 μM to 90 μM and a detection limit of 2.2 μM ¹⁰⁰.

Different dyes were electrodeposited over carbon electrode surfaces as conductive polymeric films for the fabrication of electrochemical sensors capable of detecting PR. Kuskur et al. deposited naphthol green B on the bare carbon paste electrode (CPE) surface by cyclic voltammetry in a NaOH solution¹⁰¹. When naphthol green B was electropolymerized the roughness of the surface in the graphite flakes increased which was reflected in the higher current response. Under the same conditions, using potassium ferrocyanide in KCl solution,

the poly (naphthol green B) modified CPE significantly enhanced the redox peak currents with the improvement of the fast rate of electron transfer kinetics. By CV, the modified electrode displayed sensitivity, selectivity, and stability for the determination of PR in PBS over the range of 20 μM to 70 μM with a limit of detection of 1.6 μM . Chitravathi & Munichandraiah modified a GCE with a polymeric film of Nile Blue using CV in PBS¹⁰². The formation of PNB on the surface was confirmed with the observation of a rough surface, compared to the unmodified electrode (Figure 11A(1) and A(2)). Showing an increase in the surface area improving the sensitivity in voltammetric determinations. Electron impedance spectra (EIS) revealed a semicircle with a larger diameter for the bare GCE. Charge transfer resistance (R_{ct}) values for bare GCE and PNB/GCE were 3200 and 980 $k\Omega$ respectively. Which implies that the polymeric film increases the conductivity. A wide linear range was observed from 0.2 μM to 16.2 μM with detection limit of 0.08 μM .

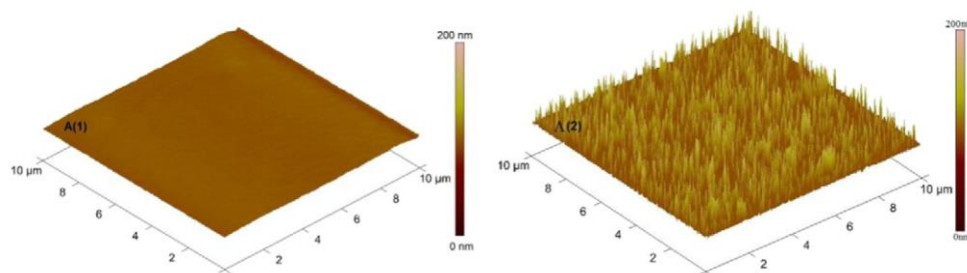


Figure 11. A(1) and A(2) 3-dimentional AFM images of the unmodified surface and Poly Nile blue modified surface respectively. Modified with permission from [102]. Copyright 2016 Elsevier.

Kaur & Srivastava developed transition metal ion-exchanged polyaniline–zeolite organic–inorganic hybrid materials for simultaneous determination of epinephrine, paracetamol, and folic acid. Among all materials, Cu^{2+} -PANI-Nano-ZSM-5 modified glassy carbon electrode exhibited the highest electro-catalytic activity. Nano-ZSM-5 was synthesized by dissolving sodium aluminate in distilled water. On the other hand, propyltriethoxysilane was mixed with tetrapropylammonium hydroxide. Both solutions were mixed and stirred under ambient conditions. Then, tetraethylorthosilicate was added and the whole mixture was transferred to autoclave. The final material was calcined, obtaining the Nano-ZSM-5. This material was converted into H^+ form, then aniline was added drop wise to the reaction mixture. Finally, ammonium peroxydisulfate was added drop-wise and stirred. PANI-Nano-ZSM-5 was cation-exchanged into with an aqueous solution of the Cu^{2+} source at 343 K¹⁰³. The Cu^{2+} -PANI-Nano-ZSM-5 suspension and Nafion were placed onto the GCE surface and dried. SEM images

showed that Cu^{2+} -PANI (Figure 12a) displays an irregular aggregated morphology. In the case of Cu^{2+} -Nano-ZSM-5 (Figure 12b), spherical particles were observed and when PANI was added, is observed that nanorods grew in the nanocomposite (Figure 12c). Cu^{2+} -PANI-Nano-ZSM-5/GCE exhibited well defined anodic and cathodic peaks, showing higher current response than bare electrode, which significantly facilitated the electron transfer rate and EIS showed a reduced semicircular domain and linear portion indicating the mixed charge transfer and diffusion kinetics-controlled reaction. Under the optimum conditions, a wide linear range was obtained from 15 nM to 800 μM with a detection limit of 8 nM¹⁰⁴.

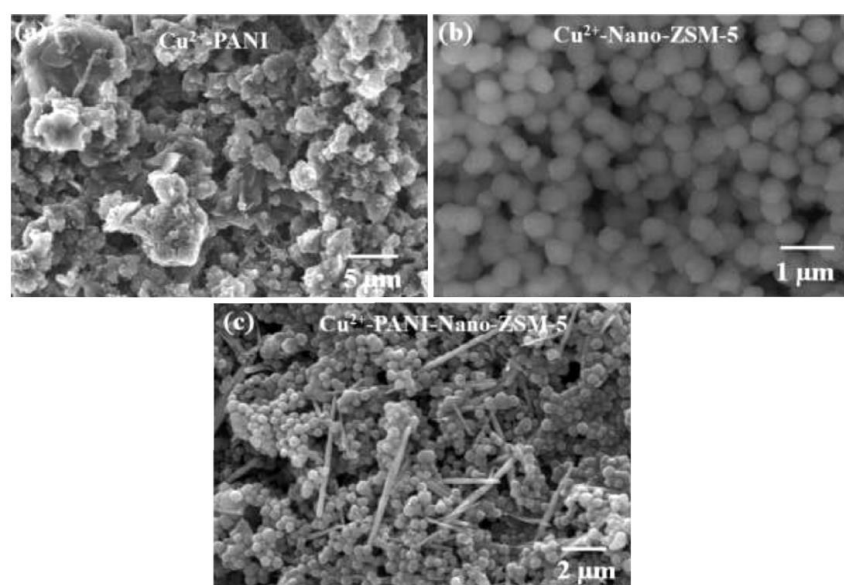


Figure 12. SEM images of (a) Cu^{2+} -PANI, (b) Cu^{2+} -Nano-ZSM-5, and (c) Cu^{2+} -PANI-Nano-ZSM-5 nanocomposite. Reproduced with permission from [104]. Copyright 2015 Elsevier.

Table 1. Summary of polymeric films, detection limits, and ranges of electrodes capable of sensing diverse pharmaceuticals.

Electrode Materials	Polymer	Manufacture Technique	Analyte	Detecting technique	LOD (uM)	Linear range (uM)	References
Poly[(3, 6-diamino-9-ethylcarbazole)]/GCE	Poly[(3, 6-diamino-9-ethylcarbazole)]	CV	E2	EIS	0.36 aM	1 aM to 10 μ M	92
MnO ₂ -Sb ₂ O ₃ /PANI/ FTO	PANI	CV	ASA	DPV	0.0002	0.0012 - 0.22868	79
PPy/sol-gel/SiO ₂ @ AuNPs MIP/Au electrode	PPy	CV	ASA	SWV	0.0002	0.001 - 0.01	80
PPy/PB/GCE	PPy	CV	PR	DPV	0.00053	0.001 - 100	95
3D-HPG/PTH/GCE	PTH	CV	MNZ	DPV	0.001	0.05 - 70	75
rGO/PPR/GCE	PPR	CV	CFX	DPV	0.002	0.002 - 0.05	88
Cu ²⁺ -PANI-Nano-ZSM-5/GCE	PANI	CV	PR	DPV	0.008	0.015 - 800	104
CS-MWCNTs+TiO ₂ NPs/PCC/nanoporous GCE	PCC	CV	Acyclovir	DPASV	0.01	0.03 - 1	84
PEBT/GCE	PEBT	CV	Acyclovir	DPV	0.012	0.03 - 0.3	83
P3MT/RGO/GCE	P3MT	CV	PR	DPV	0.025	0.2 - 2.5	96
PLum/f-MWCNTs/GCE	PLum	CV	PR	DPV	0.025	0.04 - 32.2	97
PEDOT:PSSLi/GCE	PEDOT	CA	PR	DPV	0.05	0.14 - 400	98
PEDOT:PSSLi:MWCNT/GCE	PEDOT	CA	PR	AdSDPV	0.08	1.5 - 500	
PNB/GCE	PNB	CV	PR	DPV	0.08	0.2 - 16.2	102
DMIP/CPE	Poly(AMTEOS)	CV	MNZ	DPV	0.091	0.4 - 200	73
HRP/Pol/Pt	Pol	CA	E2	DPV	0.105	0.1 - 200	91
MIP/AuNPs/GCE	PME	CV	MNZ	DPV	0.12	0.5 - 1000	74
SDS/PEB/CPE	PEB	CV	CFX	DPV	0.183	50 - 90	87
Poly(naphthol green B)/CPE	Poly(naphthol green B)	CV	PR	CV	1.6	20 - 70	101
Poly(rhodamine B)/CPE	Poly(rhodamine B)	CV	PR	CV	2.2	20 - 90	100
MWCNT/PANI/AuE	PANI	CV	PR	CA	2.9	05 - 630	99

2.2 Hydrogen peroxide

Hydrogen peroxide (H_2O_2) widely used in many fields such clinical¹⁰⁵, industrial¹⁰⁶ and environmental analysis¹⁰⁷, it is also a byproduct of several oxidases. However, the excessive use of H_2O_2 can produce side effects on human beings. Thus, monitoring this compound is of high importance¹⁰⁸. Electrochemical sensors were based on enzymes¹⁰⁹. But, recently, enzyme-free sensors have attracted increasing interest due to their high stability and cheapness¹¹⁰.

2.2.1 Enzymatic Detection

Hydrogen peroxide was sensed by a ternary nanocomposite of poly(3,4-ethylenedioxythiophene) polystyrene sulfonate (PEDOT:PSS), reduced graphene oxide (rGO) and gold nanoparticles (AuNPs) assembled with horseradish peroxidase (HRP) on a Screen Printed Gold Electrode (HRP/AuNPs/rGO/PEDOT:PSS/SPGE). PEDOT:PSS acted as an effective π - π stacking stabilizer for rGO¹¹¹. AuNPs were distributed homogeneously working as nanoscale spacers which allowed access to both faces of PEDOT:PSS and graphene sheets increasing significantly the active surface area of the electrode. Amperometric measurements using the AuNPs/rGO/PEDOT:PSS/SPGE sensed H_2O_2 concentration in a linear range from 5 μM to 400 μM and with a detection limit of 0.08 μM .

A film consisting of poly(γ -glutamic acid) modified with 3-aminothiophene (ATH- γ -PGA) was prepared together with horseradish peroxidase (HRP) and Nafion for the determination of H_2O_2 ¹¹². By cyclic voltammetry, thiophene groups present in the ATH- γ -PGA/GE were electropolymerized in acetonitrile containing LiClO_4 . Nafion/HRP/ATH- γ -PGA/GE sensors showed two linear ranges for H_2O_2 concentrations, from 0.01 nM to 10 nM and from 10 nM to 10 μM , with a detection limit of 3 pM. Chen et al. fabricated a hydrogen peroxide sensor by immobilization of HRP in an electrogenerated poly (aniline-co-N-methylthionine) film on platinum foil¹¹³. After enzyme immobilization, smaller nanoparticles appeared increasing the roughness and surface area of the electrode. Copolymer film reduced the background interference from the platinum electrode, acting also as a mediator which formed HRP (Fe^{3+}). The PAN-PNMThH film also provided a biocompatible platform for HRP immobilization. Amperometric detection of H_2O_2 showed a linear response ranging from 5.0 μM to 60.0 mM H_2O_2 with a detection limit of 3.2 μM .

A H₂O₂ sensor also based on polyaniline (PANI) together with acrylic acid (AA), ethylene glycol diglycidyl ether and Soybean seed coat peroxidase (SBP) on a Glassy carbon electrode (SBP/poly(EGDE- AA-ANI)/GCE) was developed by Torres et al¹¹⁴. The composite enhances electron transfer process, due to PANI acting as a good electronic conductor, acrylate as counter ion achieving electrical neutrality, EGDE displaying a cross-linker work and SBP catalyzing H₂O₂ reduction. The quantitative analysis of H₂O₂ using this Amperometric sensor showed a linear response in the range of 5.0 μM to 50 μM, with a detection limit of 2.2 μM

2.2.2 Enzymeless Detection

A poly(3,4-ethylenedioxythiophene) (PEDOT) together with reduced graphene oxide (rGO) were deposited on a GCE for hydrogen peroxide determination¹¹⁵. EDOT and GO were mixed in acetonitrile and drop-casted in the GCE. Cyclic voltammetry technique was applied to EDOT/GO/GCE in KCl buffer solution, where EDOT polymerized and GO was reduced. A crumpled and rough surface was observed for the PEDOT/rGO film. This morphology produced a larger electrochemically active area which enhances radical oxygen reduction reaction (ORR) activity. Wang et al. fabricated a selective and long-term stable electrode for H₂O₂ determination with prussian blue (PB) nanoparticles and poly(3,4-ethylenedioxythiophene) (PEDOT) on glassy carbon electrode (PEDOT/PBNPs/GCE)¹¹⁶. PEDOT was polymerized around the PB nanoparticles, connecting them as a covering shell. As a result, the PEDOT/ PBNPs film showed a porous grape-like microstructure. The composite enhanced the electron transfer and conductivity allowing the linear detection of H₂O₂ in concentrations ranging from 0.5 μM to 839 μM, with a detection limit of 0.16 μM. Following the same line, a PEDOT/PBNPs/Pt sensor was developed by Lete et al. resulting in an amperometric linear response for H₂O₂ concentration ranging 5 μM to 1mM with a detection limit of 1.4 μM¹¹⁷.

Electrogenerated poly(2-aminophenylbenzimidazole) (poly 2AB) and gold nanoparticles (AuNPs) coated to pencil graphite electrode (poly2AB/AuNPs/PGE) has also been used as H₂O₂ sensors¹¹⁸. AuNPs appeared as homogeneous spherical particles not only increasing the conductivity of the P2AB but also film catalyzing the reduction reaction of H₂O₂. Amperometric measurements in PBS (pH 6.5) revealed a H₂O₂ linear concentration response in the range of 0.06 mM to 100 mM with a detection limit of 36.7 μM.

Poly (methylene blue) (PMB), Ag nanocrystals (AgNCs) and graphene carbon spheres (GS) nanocomposite on glassy carbon electrode (Ag/PMB/GS/GCE) were used for hydrogen peroxide detection¹¹⁹. GS had wrinkled texture, showing a rough surface with pores that favors electron transport. The thin layer of PMB acted as a mediator absorbing and binding the Ag⁺ ions. The morphology of AgNCs presented dendritic-like structures. The carbon spheres act as nano-spacers preventing the aggregation of graphene, while, poly(MB) benefits the crystals growth during the reduction of AgNCs. Ag/PMB/GS/GCE amperometric sensor showed a linear response for H₂O₂ concentration ranging from 0.5 μM to 1112 μM with a detection limit of 0.15 μM.

Copolymer poly(pyrrole-3-carboxylic acid) (PPy3C) - polypyrrole (PPy) on mesoporous platinum (MPrPt) at boron-doped diamond (BDD) was used for nonenzymatic, free of oxygen interference sensing of hydrogen peroxide¹²⁰. After Pt was deposited, mesoporous and snowflake-like nanoclusters were formed. Electrodeposited copolymer increased the porosity of the structure, allowing molecules to permeate through the polymer film. The PPy3C-PPy/MPrPt/BDD electrode showed an amperometric linear response for H₂O₂ concentration that ranged from 5 μM to 49 mM with a detection limit of 2 μM. The enhancement of the current peak should come from the increasing conductivity by the copolymer and electrocatalytic reduction of PtO₂/PtO by H₂O₂.

Table 2. Summary of polymeric films, detection limits, and ranges of electrodes capable of sensing hydrogen peroxide.

Electrode Materials	Polymer	Manufacture Technique	Analytes	Detecting technique	LOD (uM)	Linear range (uM)	References
Nafion/HRP/ATh- γ -PGA/GE	ATh- γ -PGA	CV	H ₂ O ₂	DPV	3.0 pM	0.00001 - 0.010	112
HRP/AuNPs/rGO/PEDOT:PSS/SPGE	PEDOT:PSS		H ₂ O ₂	CA	0.08	5 - 400	111
Ag/PMB/GS/GCE	PMB	CV	H ₂ O ₂	CA	0.15	0,5 - 1112	119
PEDOT/PBNPs/GCE	PEDOT	CA	H ₂ O ₂	CA	0.16	0.5 - 839	116
PEDOT/PBNPs/Pt	PEDOT	SV	H ₂ O ₂	CA	1.4	5 - 1000	117
PPy3C-PPy/MPrPt/BDD	PPy3C-PPy	CV	H ₂ O ₂	CA	2.0	5 - 49000	120
SBP/poly(EGDE- AA-ANI)/GCE	PANI	radical polymerization	H ₂ O ₂	CA	2.2	5.0 - 50	114
HRP/PAN-PNMThH	PAN-PNMThH	CV	H ₂ O ₂	CA	3.2	5 - 60000	113
poly2AB/AuNPs/PGE	poly2AB	CV	H ₂ O ₂	CA	36.7	60 - 100000	118

2.3 Nitrites

Nitrites are important in the nitrogen cycle and in food preservation, as well as a fertilizing agent^{121,122}. However, when ingested, it causes the oxidation of haemoglobin into methaemoglobin in blood, avoiding this protein to bind with oxygen molecule¹²³. Nitrite can react with degradation products of meat forming nitrosamines which are carcinogen compounds¹²⁴. The World Health Organization reported that nitrite levels in water should stay below 3mg/L¹²⁵. Thus, precise determination of nitrite is of high importance for environment and human health.

Poly(3,4-ethylenedioxythiophene) (PEDOT) and carbon quantum dots (CQDs) has been used for nitrite sensing by modifying a glassy carbon electrode (CQDs/PEDOT/GCE)¹²⁶. Direct electrochemical polymerization of the composite was performed by potentiostatic methods in an aqueous solution containing CQDs and EDOT. The CQD-PEDOT film was rough and lumpy with small pores throughout the film, enlarging the surface area. The nanocomposite act as a promoter to enhance the kinetics of the electrochemical oxidation process which effectively electro-catalyzes oxidation of nitrite.

The CQDs/PEDOT/GCE showed a nitrite linear response with a range from 0.5 μM to 1110 μM and a limit of detection of 88 nM. A similar approach was followed by Wang et al. by modifying a CGE with poly(3,4-ethylenedioxythiophene) doped with nano-sized hydroxyapatite (nHAp/PEDOT/GCE)¹²⁷. The electrodeposition was carried out under potentiostatic regime in a solution containing nHAp and EDOT. The nHAp/PEDOT film exhibited a rough three-dimensional reticular structure. EIS showed a lower Rct for nHAp/PEDOT/GCE if compared to the one obtained in bare GCE, attributed to the large surface area and enhanced conductivity of the nanocomposite. Linear amperometric response for nitrite concentrations ranged from 0.25 μM to 1.05 mM with a limit of detection of 83 nM. A multilayered film of electrogenerated poly(3,4-ethylenedioxythiophene)/poly(thiomethyl 3,4-ethylenedioxythiophene)/gold nanoparticle (PEDOT-SH/PEDOT/Au) nanocomposite was fabricated by Ge et al.¹²⁸ Figure 13 shows a schematic illustration for the electrogenerated PEDOT-SH/PEDOT/Au/GCE sensor preparation and nitrite sensing.

PEDOT film exhibited nanofiber structures which formed a porous network. PEDOT-SH thickened the nanofibers and formed block structures. AuNPs were distributed uniformly on the porous network directed by bonding interactions with thiol groups. Au/PEDOT-SH/PEDOT/GCE sensor exhibited a low detection limit of 51 nM and two amperometric linear ranges from 0.15 mM to 1mM and from 1 mM to 16 mM, for nitrite concentration. Zuo et al. designed a sensitive and selective nitrite sensor based on phosphovanadomolybdates $H_6[PMo_9V_3O_{40}]$, poly(ethylenimine), poly(3,4-ethylenedioxythiophene) and gold nanoparticles on glassy carbon (AuNP/PEDOT/ PMo_9V_3 / PEI/GCE)¹²⁹. After GCE modification, a rough surface was obtained showing a uniform distribution of gold nanoparticles in the polymer film. This amperometric sensor showed a linear range of nitrite concentration and LOD of 2.5 nM - 1.43 mM and 1.0 nM, respectively. These outstanding results might be related to PEDOT π -conjugation and the presence of sulfur atoms, which chemically bond with the well-distributed gold nanoparticles, improving the electrical conductivity and electron transfer; while, polyoxometalates act as a proton and electron reservoir in the electrocatalytic process. Together, they enhance greatly the electrocatalytic activity.

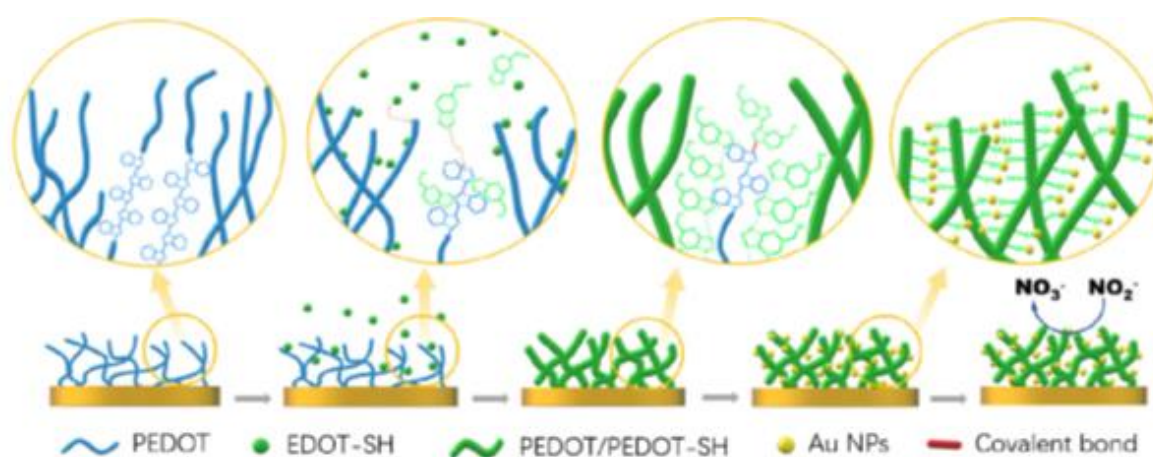


Figure 13. The growth process of PEDOT/PEDOT-SH/Au on electrode surface. Reproduced with permission from [128]. Copyright 2020 Springer

Poly(1,5-diaminonaphthalene) together with palladium nanoparticles and Multiwalled Carbon Nanotubes (MWCNTs) on Glassy Carbon Electrode (PdNPs-poly(1,5-DAN)/MWCNTs/GCE) exhibited a high analytical performance for nitrite detection¹³⁰. An amperometric sensor for nitrite showed a peak current proportional to its concentration in a linear range of 0.25 μ M to 0.1 mM, with a limit of detection of 0.08 μ M. Nitrite was determined, as well,

using a glassy carbon electrode (GCE) modified with graphene oxide, polypyrrole (PPy) and cobalt nanostructures (CoNS/GO/PPy/GCE)¹³¹. The GO/PPy nanocomposite showed a porous two-dimensional nanoflake structure. Cobalt NS revealed a flower-like crystal structure with open-nanoporous that increase significantly the active surface area ensuring unhindered diffusion of ions and redox substances. Under optimum conditions, using amperometry, nitrite concentration showed two different linear ranges, from 1.0 μM to 3.2mM and 6.8 mM to 12mM with a lower detection limit of 15 nM and a response time of 1 s.

Table 3. Summary of polymeric films, detection limits, and ranges of electrodes capable of sensing nitrites.

Electrode Materials	Polymer	Manufacture Technique	Analytes	Detecting technique	LOD (uM)	Linear range (uM)	References
AuNP/PEDOT/PMO ₉ V ₃ /PEI/GCE	PEDOT	CV	nitrite	CA	0.001	0.0025 - 1430	¹²⁹
CoNS/GO/PPy/GCE	PPy	CV	nitrite	CA	0.015	1.0 - 3200	¹³¹
PdNPs/poly(1,5-DAN)/MWCNTs/GCE	poly(1,5 DAN)	CV	nitrite	CA	0.08	0.25 - 100	¹³⁰
nHAp/PEDOT/GCE	PEDOT	CA	nitrite	CA	0.083	0.25 - 1050	¹²⁷
CQDs/PEDOT/GCE	PEDOT	CA	nitrite	CA	0,088	0.5 - 1110	¹²⁶
Au/PEDOT-SH/PEDOT/GCE	PEDOT-SH/PEDOT	CV	nitrite	CA	51	150 - 1000	¹²⁸

2.4 Phenolic Compounds

Phenolic compounds are important chemicals used in several industries such as synthetic resins, plants¹³², paints, textile, plastic¹³³, pharmaceutical, petroleum and mine discharges¹³⁴. However, they are considered as a major class of pollutants due to its high toxicity, carcinogenicity and low biodegradability¹³⁵. The World Health Organization (WHO) has determined 1 µg/L as the maximum concentration allowed in drinking water¹³⁶. These compounds can cause severe diseases e.g., methemoglobinemia¹³⁷, drowsiness¹³⁸, and nausea¹³⁹. Therefore, methods for the determination of these compounds in long-term and real-time are of great significance. It is then that electrochemical methods, with low cost and rapid analysis, take importance for practical applications¹⁴⁰. Moreover, conducting polymer modified electrodes exhibit good sensitivity, selectivity and reproducibility¹⁴¹.

Voltammetric determination of (2R,3S)-2-(3,4-dihydroxyphenyl)-3,4-dihydro-2H-chromene-3,5,7-triol (catechin) was performed using a glassy carbon electrode doped with poly(hydroxymethylated-3,4-ethylenedioxythiophene) (PEDOTM) and carboxylic group functionalized single-walled carbon nanotubes (f-SWCNTs)¹⁴². After potentiostatic deposition of PEDOTM on GCE, f-SWCNTs were drop-casted and dried at room temperature. The nodular and highly porous morphology of the f-SWCNTs/PEDOTM/GCE provided a large electroactive area which showed a linear behavior for catechin concentration, in PBS (pH 7.00), ranging from 0.039 µM to 40.84 µM with a detection limit of 0.013 µM. The f-SWCNTs/PEDOTM film highly increased the active surface area for the adsorption of catechin accelerating the electron transfer between electrode and solution, which boosted the current response and improved the sensitivity. Moreover, one-dimensional electrogenerated poly(3,4-ethylenedioxythiophene)-graphene composite (PEDOT-Gr) were used for the detection of resorcinol (RC), hydroquinone (HQ) and catechol (CC)¹⁴³. The graphene sheets showed atomic defects covering the edges and basal planes which produced high nucleation density allowing the formation of PEDOT structures with a 1D morphology in the edges of the sheets. 1D PEDOT-Gr/Ta sensor showed well-defined peaks at 12 mV (HQ), 120 mV (CC) and 512 mV (RC) with linear ranges of 5–250 µM, 0.4–350 µM and 6–2000 µM and detection limits of 0.06 µM, 0.08 µM and 0.16 µM, respectively. The high electron affinity and aromaticity of thiophene with the high conductivity of graphene nanosheets and the specific electron transfer

properties accessible only to 1D material, all together showed exceptional ability to adsorb and capture electrons of multiple analytes and discriminate between them.

Sensitive and selective sensing of catechol (CC) and hydroquinone (HQ) was fabricated by Kuskur et al. with electrodeposited poly(Naphthol green B) modified carbon paste electrode (poly(NG B)/CPE)¹⁴⁴. The morphology changed from irregularly shaped micrometer-sized flakes of graphite to uniform arrangement of poly (NG B) molecules on the surface of the electrode. The highest electrocatalytic activity was achieved at tenth cycle. The bare electrode showed amalgamated and indistinguishable signals for CC and HQ while poly(NG B)/CPE showed two clearly separated anodic peak potentials at 0.207 V (CC) and 0.0821 V (HQ). Under optimal conditions, the modified CPE is capable of detecting CC and HQ in the 0.20 μM to 90 μM concentration range with a detection limit of 0.19 μM and 0.20 μM , respectively. Improved detection for modified CPE raises due to formation of stable redox active layers and high electron transfer efficiency of poly(NG B) acting as mediators for electrocatalysis of biological compounds.

A selective non-enzymatic sensor for catechol (CC) determination was developed using Copper-polypyrrole modified GC electrode (Cu-PPy/GCE)¹⁴⁵. SEM images revealed globular PPy structures resulting in a microporous morphology. While, Cu deposits showed pinecone-like morphologies on the micropores of PPy surface. Under optimized conditions, DPV measurements in PBS (pH = 7.0) gave a wide linear range from 10 μM to 1750 μM with a detection limit of 1.17 μM ; while, amperometric measurements showed a linear range from 0.05 μM to 1000 μM with 0.010 μM as LOD (see Figure 14a and b). The high electrocatalytic behavior and selectivity of Cu-PPy/GCE towards CC is attributed to the formation of a five member Cu(II)-o-quinolate intermediate complex and the CC oxidation to o-quinone through the reduction of Cu (II) to Cu (I) that enhances the electron transference (Figure 14c).

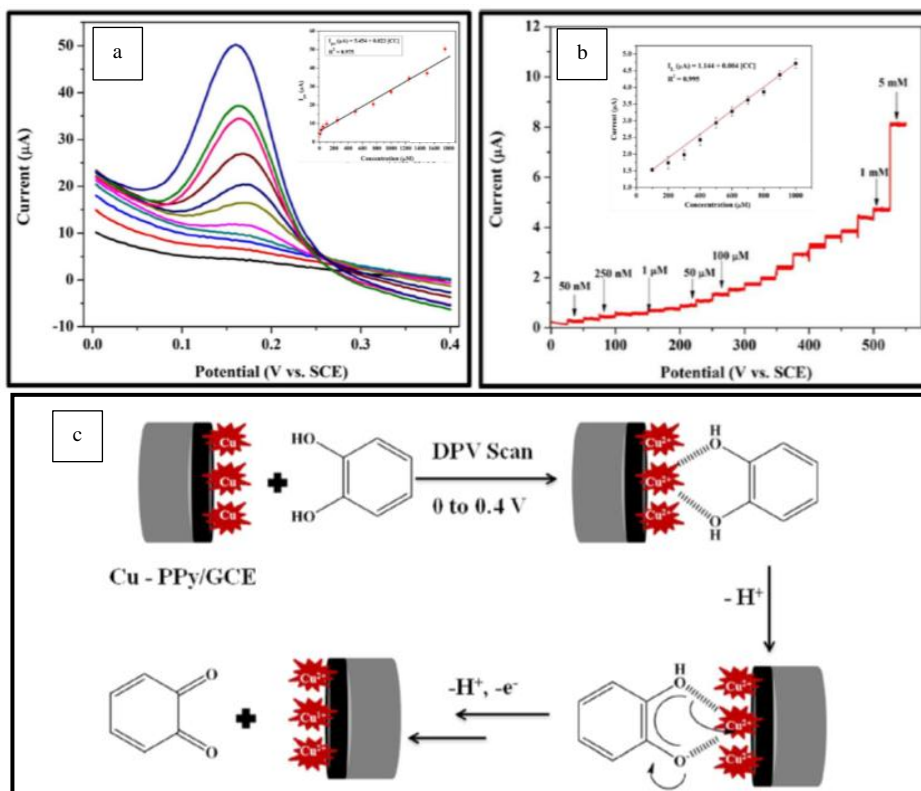


Figure 14. (a) Differential pulse voltammograms at various CC concentrations at Cu-PPy/GCE in 0.1 M PBS (pH = 7.0) and Inset: the corresponding calibration plot. (b) Chronoamperogram for the sequential addition of CC at various concentrations at 0.3 V. Inset: denote the corresponding calibration plot. (c) Formation of five membered ring with Cu(II) and CC and further oxidation of CC at Cu-PPy/GCE. Modified with permission from [145]. Copyright 2017 Electrochemical Society.

Table 4. Summary of polymeric films, detection limits, and ranges of electrodes capable of sensing phenolic compounds.

Electrode Materials	Polymer	Manufacture Technique	Analytes	Detecting technique	LOD (uM)	Linear range (uM)	References
<i>f</i> -SWCNTs/PEDOTM/GCE	PEDOTM	CA	catechin	CV	0.013	0.039 - 40.84	142
poly(NG B)/CPE	poly(NG B)	CV	HQ	DPV	0.01	0.1 - 110	144
			CC	CV	0.19	0.20 - 90	
			HQ	CV	0.20	0.20 - 90	
Cu-PPy/GCE	PPy	CA	CC	CA	0.010	0.05 - 1000	145
				DPV	1.17	10 - 1750	
1D PEDOT-Gr/Ta	PEDOT	CV	HQ	DPV	0.06	5 - 250	143
			CC	DPV	0.08	0.4 - 350	
			RC	DPV	0.16	6 - 2000	

2.5 Nitroaromatic Compounds

Nitroaromatic compounds are pollutants that commonly infiltrate soil and groundwater because of its usage in industries of rubber, dye, pharma, detergent, resin, paper, and widely in the armament industry as explosives^{146,147}. On humans, the toxicological impact is high because they persist long periods, producing several health problems such skin damage and necrosis¹⁴⁸. As they have nitro-substituted groups attached to an aromatic are quite chemically stable and poorly biodegradable in the environment¹⁴⁹. However, the advantage of the easily reducible nitro groups allows for the application of electrochemical methods for their detection showing good sensitivity and selectivity, and fast response¹⁵⁰.

Furthermore, modifying electrodes with polymers and nanoparticles had proven to result in a great increase in the recognition of analytes and stability of the electrodes¹⁵¹.

Nitroaromatic explosive materials such 2,4,6-trinitrotoluene (TNT), 2,4-dinitrotoluene (DNT) and 2,4,6-trinitrophenylmethylnitramine (tetryl) were detected using glassy carbon electrode coated with electrogenerated poly(o-phenylenediamine–aniline) and gold nanoparticles (AuNp/ P(o-PDA-co-ANI)/GCE)¹⁵². Poly(o-PDA) film was able to catalyze nitroaromatic compounds, however, the coating peeled off the surface after several measurements. In the case of PANI film, it exhibited stability through measurements, but it was non-reactive to nitroaromatic compounds. On the other hand, P[o-PDA-co-ANI] exhibited both stability and electroactivity, in which nitroaromatic compounds were detected through π -acceptor/donor interactions. AuNp's provided increased binding, because s -/ π -donor amine/aniline groups could link gold nanoparticles interacting with the electron-poor nitroaromatic compounds. Linear responses were observed for 2,4,6-trinitrotoluene (TNT) ranging from 2.5 mg L⁻¹ to 40 mg L⁻¹ with a LOD of 2.1 mg L⁻¹, for 2,4-dinitrotoluene (DNT) ranging from 2.0 mg L⁻¹ to 40 mg L⁻¹ with a LOD of 1.28 mg L⁻¹, and for tetryl ranging from 5.0 mg L⁻¹ to 100 mg L⁻¹ with a LOD of 3.8 mg L⁻¹. Potentiodynamic deposition of polyalizarin red on glassy carbon electrode (PAR/GCE) was proposed by Chen et al. for detection of nitrofurazone, nitrofurantoin and furazolidone. GCE has a mirror-like surface, however after PAR deposition, it turned uniformly granular. The reduction peak current of nitrofurazone using PAR/GCE in HAc-NaAc buffer (pH 5.0) was 2.47 times higher than bare GCE. DPV sensor showed a peak current proportional to the concentration in the range of 3.0 μ M–50.0 μ M and 50.0 μ M–200.0 μ M, having a detection limit of 0.33 μ M for nitrofurazone. Further analysis of furantoin and furazolidone showed linear ranges of 10 μ M–40 μ M and 50 μ M–140 μ M,

respectively, with corresponding detection limits of 0.73 μM and 1.56 μM ¹⁵³. Nitrophenol isomers were sensed using graphite electrode coated with poly(p-aminobenzenesulfonic acid) (poly(p-ABSA)) film. Electrochemical potentiodynamic deposition was carried out using a PBS (pH 5.00) solution containing p-ABSA. (o-, m- and p-NP) isomers were simultaneously determined at 0.119 V, -0.125 V and 0.027 V (vs. SCE) using a semi-derivative technology which improved the resolution and enhanced the sensitivity of CV curves. Linear ranges for the oxidation peaks of the intermediate products of nitrophenol were 3 mM - 800 mM for o-NP and 3 mM - 700 mM for both m-NP and p-NP. Sensitivity and detection limits for o-NP (0.28 mM), m-NP (0.5mM) and p-NP (0.3 mM) were attributed to the favorable electrocatalytic activity of poly(p-ABSA) towards the oxidation of hydroxyl aminophenol¹⁵⁴. Nitrofurantoin (NFT), nitrofurazone (NFZ), furaltadone (FTD), and furazolidone (FZD) were successfully determined using a screen-printed carbon electrode coated with overoxidized multi-walled carbon nanotubes and poly(melamine) (PME/MWCNT*/SPCE)¹⁵⁵. Multifunctional melamine was electropolymerized in HCl solution by cyclic voltammetry on MWCNT modified electrodes possibly leading to the formation of microporous structures. While the bare SPCE is very hydrophobic, with a water contact angle of 136°, the PME/MWCNT*/SPCE displayed a reduced hydrophobic characteristic with a value of 52.1°. The linear relation from peak current and concentration for NFT, FZD and NFZ ranged for all from 0.05 μM to 2.0 μM with LODs of 0.012 μM , 0.007 μM and 0.006 μM , respectively. The linear response for FTD was higher going from 0.05 μM to 5.0 μM and a LOD of 0.014 μM . We have designed a series of microporous polymer networks (MPNs) based on multifunctional carbazole monomers on GCE for the analysis of 1,3,5-trinitrobenzene (TNB). The monomers, which differed mostly in the number of carbazole units, were electrodeposited by potentiostatic methods in acetonitrile/dichloromethane non-aqueous solution containing tetrabutylammonium perchlorate (TBAP). As the monomers possess multiple carbazole functions around a rigid core unit, the resultant film is a three-dimensional network with permanent microporosity. Direct measurement of the specific surface area was determined for the MPNs using krypton gas sorption measurements followed by data analysis using the Brunauer–Emmett–Teller (BET) equation reaching values up to 1297 m^2g^{-1} . The electron-rich MPN surface interacts with electron-poor nitroaromatic analytes via π - π interactions boosting the sensitivity of the electrode, which is closely related to the specific area, showing a current increase of 182 between modified and nonmodified GCE¹⁵⁶. Similar works have also been published where it was clearly demonstrated the importance of

producing high microporosity films, starting from different multifunctional monomers, for the sensitivity boosting of modified electrodes in the detection of nitroaromatics^{157–159}.

A gold electrode (GE) modified with 3,5-diamino-1,2,4-triazole (35DT) was used for sensing 4-nitrophenol (4NP). Poly(35DT)/GE electrode was built by cyclic voltammetry in 35DT solution. The electrode, contrary to what was expected, suffered a decrease in the faradaic current because the Au surface was slightly blocked after the coating. However, with the use of a proper supporting electrolyte solution (SE) and pH (acetate buffer; pH 4.5) the anodic current of the modified electrode compared to the bare one was 49.2 times higher (see Figure 15). Using DPV for performing the calibration curve, the linear response obtained for the concentration of 4NP ranged from 0.24 μM to 130.6 μM with a detection limit of 0.09 μM ¹⁶⁰.

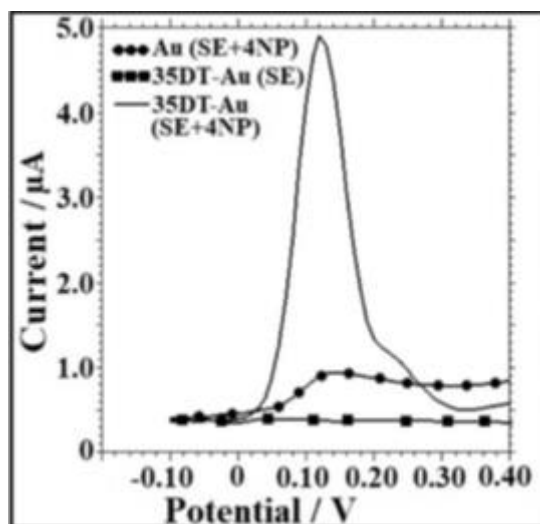


Figure 15. DPVs, with (solid circle) the bare electrode in SE and 50 μM 4NP, with (square line) the poly(35DT)/Au electrode in SE and (solid line) the presence of poly(35DT)/Au electrode in SE and 50 μM 4NP. Modified with permission from [160]. Copyright 2019 Wiley - VCH Verlag GmbhH & Co.

Arulraj et al. fabricated an electrogenerated nano polypyrrole/sodium dodecyl sulphate (ENPPy/SDS) film for the determination of *p*-nitrophenol (*p*-NP)¹⁶¹. Oxidation peak current showed a linear detection in the range of 0.1 nM - 100 μM with a LOD of 0.1 nM and sensitivity of 4.4546 $\mu\text{A } \mu\text{M}^{-1}$. The catalytic effect of ENPPy/SDS film can be explained by the electrochemical treatment in which the initial globular structure (Figure 16a) is nano cracked and decreases particle size of the polymer (Figure 16b). Cracks allow *p*-NP to diffuse into the polymer matrix through capillary action and act as micro electrochemical cells catalyzing the reaction.

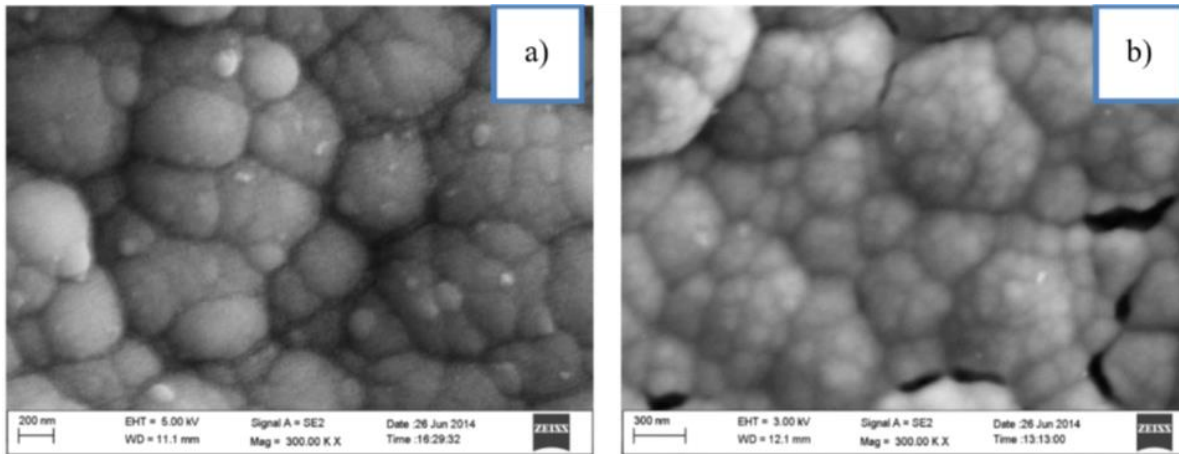


Figure 16. FESEM images of polypyrrole/sodium dodecyl sulphate film, a) before electrochemical treatment, b) after electrochemical treatment showing nano cracks. Modified with permission from [161]. Copyright 2015 Elsevier.

Table 5. Summary of polymeric films, detection limits, and ranges of electrodes capable of sensing nitroaromatic compounds.

Electrode Materials	Polymer	Manufacture Technique	Analytes	Detecting technique	LOD (uM)	Linear range (uM)	References
ENPPy/SDS/GCE	ENPPy	CV	<i>p</i> -NP	SWV	0.0001	0.0001 - 100	161
Poly(35DT)/GE	Poly(35DT)	CV	4-NP	DPV	0.09	0.24 - 130.6	160
poly(<i>p</i> -ABSA)/GrE	poly(<i>p</i> -ABSA)	CV	<i>o</i> -NP	SDV	0.28	03 - 800	154
			<i>p</i> -NP	SDV	0.3	03 - 700	
			<i>m</i> -NP	SDV	0.5	03 - 700	
PAR/GCE	PAR	CV	NF	DPV	0.33	3.0 - 50	153
			NIT	DPV	0.73	10.0 - 40	
			FL	DPV	1.56	50 - 140	
PME/MWCNT*/SPCE	PME	CV	NFZ	DPV	0.006	0.05 - 2.0	155
			FZD	DPV	0.007	0.05 - 2.0	
			NFT	DPV	0.012	0.05 - 2.0	
			FTD	DPV	0.014	0.05 - 5.0	
AuNp/P(<i>o</i> -PDA-co-ANI)/GCE)	P(<i>o</i> -PDA-co-ANI)	CV	DNT	CV	7.03	11 - 220	152
			TNT	CV	9.25	11 - 176	
			Tetryl	CV	13.23	14 - 348	

Conclusions and Recommendations

Conclusions

Electrochemical polymeric sensors have been developed for versatile and selective detection of different organic and inorganic compounds such phenolic compounds, nitrites, pharmaceuticals, nitroaromatic compounds and hydrogen peroxide. The most used monomers are derivatives of pyrroles, EDOTs and conjugated organic dyes because of its capacity to produce polymers with high conductivity, large surface area and improvement in electron transfer kinetics, which enhances electrocatalytic activity of the sensor. These polymers have the advantage that they can be coupled with many other materials such multi-walled nanotubes, capable of increasing adsorption of analytes or enzymes, which rises sensitivity and allows biocompatibility. These composites show excellent performance due to synergetic effects of the polymer with the other components, demonstrating a high improvement in sensitivity, selectivity and stability.

Cyclic voltammetry and chronoamperometry are used commonly in the synthesis of the polymeric film, because with these techniques, the thickness can be regulated due to number of cycles or time. The composite is formed when the other materials are electropolymerized as well, or drop-casted. Frequently, graphene oxide is reduced before drop-casting, while materials like nanoparticles or nanotubes can be added to the monomer solution before polymerization, which allows its direct incorporation. MIPs, are created in a similar way, the analyte is added to the solution of the monomer and when the electropolymerization takes place, the molecule acts as a template. Which artificially synthesizes receptor structures with specific recognition, increasing highly the selectivity of the sensor.

These polymeric sensors, as instrumental methods, display limits of detection that can reach attomolar concentrations, which satisfy the detection requirements in environmental monitoring. Other important advantage is the wide linear ranges, been as large as changing the order of magnitude without affecting the linearity of the statistical analysis.

Nowadays, electrochemical polymeric sensors play important roles in online, in situ, real time and noninvasive determination of aqueous pollutants. However, there are still challenges as well as developments for polymeric sensors, most of the films form one or bidimensional structures, which can form high roughness and large surface area by meso- and macroporosity. Nevertheless, recent efforts point to the development of tridimensional networks with high

microporosity capable of enhancing not only conductivity, but also selectivity and adsorption increasing the mechanical properties of the film as well.

Recommendations

The initial goal of this undergraduate thesis was to sense and determine emergent residues using a sensor based on double, triple and tetra functional carbazoles on GCE. However, due to the global health emergency caused by the Sars-CoV2 virus, the experimental research had to stop changing its objectives to a state-of-the-art review.

In this context, for further working with polymeric films, it is important to optimize the deposition of the monomers. The technique of deposition is fundamental, depending on the monomer, such carbazoles. Coulometry might be a good option, as charge is the parameter that determines the growing of the film. For polymers like PANI, cyclic voltammetry is a useful technique. The deposition solution plays an important role, because depending on the solubility of the monomer, mixtures of solvents should be used. Nevertheless, if the solution solubilizes too much the monomer, is highly possible that the polymer will not stay deposited in the electrode, because the oligomers dissolve in the solution. On the other hand, if the monomer is not soluble at all on the solution, the concentration able to be polymerized decreases.

The target molecule is fundamental at the moment of deciding if a composite should be used or not. In the case of nitroaromatic compounds, carbazoles are a great option, because the film highly enhances the conductivity. However, metals are poor sensed, at the point that bare GCE shows better electron transfer kinetics. In that case, a combination of monomers or nanoparticles can overcome this issue.

References

1. Badihi-Mossberg, M., Buchner, V. & Rishpon, J. Electrochemical biosensors for pollutants in the environment. *Electroanalysis* **19**, 2015–2028 (2007).
2. Honeychurch, K. C. & Hart, J. P. Screen-printed electrochemical sensors for monitoring metal pollutants. *TrAC - Trends Anal. Chem.* (2003). doi:10.1016/S0165-9936(03)00703-9
3. Lin, C.-Y., Balamurugan, A., Lai, Y.-H. & Ho, K.-C. A novel poly(3,4-ethylenedioxythiophene)/iron phthalocyanine/multi-wall carbon nanotubes nanocomposite with high electrocatalytic activity for nitrite oxidation. *Talanta* **82**, 1905–1911 (2010).
4. Endo, T., Yanagida, Y. & Hatsuzawa, T. Quantitative determination of hydrogen peroxide using polymer coated Ag nanoparticles. *Meas. J. Int. Meas. Confed.* (2008). doi:10.1016/j.measurement.2008.03.004
5. Tohidinia, M., Farsadrooh, M., Bahmanzadeh, S., Sabbaghi, N. & Noroozifar, M. Poly(quercetin)-bismuth nanowires as a new modifier for simultaneous voltammetric determination of dihydroxybenzene isomers and nitrite. *RSC Adv.* **8**, 1237–1245 (2018).
6. Kou, L. J., Liang, R. N., Wang, X. W., Chen, Y. & Qin, W. Potentiometric sensor for determination of neutral bisphenol A using a molecularly imprinted polymer as a receptor. *Anal. Bioanal. Chem.* (2013). doi:10.1007/s00216-013-6877-2
7. Paitan, Y. *et al.* Monitoring aromatic hydrocarbons by whole cell electrochemical biosensors. *Anal. Biochem.* **335**, 175–183 (2004).
8. Green, L. C. *et al.* Analysis of nitrate, nitrite, and [¹⁵N]nitrate in biological fluids. *Anal. Biochem.* (1982). doi:10.1016/0003-2697(82)90118-X
9. Bernal, J. L., Del Nozal, M. J., Martin, M. T. & Jiménez, J. J. Possibilities of gas chromatography-atomic emission detection in pesticide multiresidue analysis. Application to herbicide analysis in soils. *J. Chromatogr. A* (1996). doi:10.1016/S0021-9673(96)00200-2
10. Jenkins, A. L., Yin, R. & Jensen, J. L. Molecularly imprinted polymer sensors for pesticide and insecticide detection in water. *Anal. (Cambridge, United Kingdom)* **126**, 798–802 (2001).

11. Lagarde, F. & Jaffrezic-Renault, N. Cell-based electrochemical biosensors for water quality assessment. *Anal. Bioanal. Chem.* **400**, 947–964 (2011).
12. Pichon, V. & Chapuis-Hugon, F. Role of molecularly imprinted polymers for selective determination of environmental pollutants-A review. *Anal. Chim. Acta* **622**, 48–61 (2008).
13. Thévenot, D. R., Toth, K., Durst, R. A. & Wilson, G. S. Electrochemical biosensors: Recommended definitions and classification. *Biosens. Bioelectron.* (2001). doi:10.1016/S0956-5663(01)00115-4
14. Lobnik, A., Turel, M. & Urek, Š. *Optical chemical sensors: design and applications.* (InTech Rijeka, Croatia, 2012). doi:10.5772/31534
15. Scheller, F. W. *et al.* Biosensors: Fundamentals, applications and trends. *Sensors Actuators B. Chem.* **4**, 197–206 (1991).
16. *Encyclopedia of Applied Electrochemistry. Encyclopedia of Applied Electrochemistry* (2014). doi:10.1007/978-1-4419-6996-5
17. Janata, J. Peer Reviewed: Centennial Retrospective on Chemical Sensors. *Anal. Chem.* (2001). doi:10.1021/ac012402a
18. Wang, J. *Analytical Electrochemistry, Third Edition. Analytical Electrochemistry, Third Edition* (2006). doi:10.1002/0471790303
19. Stradiotto, N. R., Yamanaka, H. & Zanoni, M. V. B. Electrochemical sensors: A powerful tool in analytical chemistry. *Journal of the Brazilian Chemical Society* (2003). doi:10.1590/S0103-50532003000200003
20. Guinovart, T., Parrilla, M., Crespo, G. A., Rius, F. X. & Andrade, F. J. Potentiometric sensors using cotton yarns, carbon nanotubes and polymeric membranes. *Analyst* (2013). doi:10.1039/c3an00710c
21. Coyle, S., Curto, V. F., Benito-Lopez, F., Florea, L. & Diamond, D. Wearable Bio and Chemical Sensors. in *Wearable Sensors: Fundamentals, Implementation and Applications* (2014). doi:10.1016/B978-0-12-418662-0.00002-7
22. Ghosh, S. *et al.* Extremely high thermal conductivity of graphene: Prospects for thermal management applications in nanoelectronic circuits. *Appl. Phys. Lett.* (2008).

doi:10.1063/1.2907977

23. Shao, Y. *et al.* Graphene based electrochemical sensors and biosensors: A review. *Electroanalysis* (2010). doi:10.1002/elan.200900571
24. Stetter, J. R., Penrose, W. R. & Yao, S. Sensors, Chemical Sensors, Electrochemical Sensors, and ECS. *J. Electrochem. Soc.* (2003). doi:10.1149/1.1539051
25. Skotheim, T. A. & Reynolds, J. R. *Handbook of Conducting Polymers: Conjugated Polymers Processing and Applications. Chemistry & ...* (2007).
26. Rattan, S., Singhal, P. & Verma, A. L. Synthesis of PEDOT:PSS (poly(3,4-ethylenedioxythiophene))/poly(4-styrene sulfonate)/NGPs (nanographitic platelets) nanocomposites as chemiresistive sensors for detection of nitroaromatics. *Polym. Eng. & Sci.* **53**, 2045–2052 (2013).
27. Wang, Y., Liu, A., Han, Y. & Li, T. Sensors based on conductive polymers and their composites: a review. *Polymer International* (2020). doi:10.1002/pi.5907
28. Dominguez-Renedo, O., Alonso-Lomillo, M. A. & Arcos-Martinez, M. J. Determination of Metals Based on Electrochemical Biosensors. *Crit. Rev. Environ. Sci. Technol.* **43**, 1042–1073 (2013).
29. Evans, D. H. Review of voltammetric methods for the study of electrode reactions. in *Microelectrodes: Theory and Applications* 17–32 (Springer, 1991). doi:10.1007/978-94-011-3210-7_2
30. Lenik, J. Cyclodextrins Based Electrochemical Sensors for Biomedical and Pharmaceutical Analysis. *Curr. Med. Chem.* (2016). doi:10.2174/0929867323666161213101407
31. Kissinger, P. T. & Heineman, W. R. Cyclic voltammetry. *Journal of Chemical Education* (1983). doi:10.1021/ed060p702
32. Mabbott, G. A. An introduction to cyclic voltammetry. *Journal of Chemical Education* (1983). doi:10.1021/ed060p697
33. Kawagoe, K. T., Zimmerman, J. B. & Wightman, R. M. Principles of voltammetry and microelectrode surface states. *Journal of Neuroscience Methods* (1993). doi:10.1016/0165-0270(93)90094-8

34. Henstridge, M. C., Laborda, E., Rees, N. V. & Compton, R. G. Marcus-Hush-Chidsey theory of electron transfer applied to voltammetry: A review. *Electrochim. Acta* (2012). doi:10.1016/j.electacta.2011.10.026
35. Bockris, J. Electrochemical methods — Fundamentals and applications Allen J. Bard and Larry R. Faulkner, Wiley, New York, 1980, xviii + 718 pp., £ 14.70. *J. Electroanal. Chem.* (1981). doi:10.1016/0368-1874(81)87163-8
36. Rifkin, S. C. & Evans, D. H. General Equation for Voltammetry with Step-Functional Potential Changes Applied to Differential Pulse Voltammetry. *Anal. Chem.* (1976). doi:10.1021/ac50005a050
37. Simões, F. R. & Xavier, M. G. Electrochemical Sensors. in *Nanoscience and its Applications* (2017). doi:10.1016/B978-0-323-49780-0.00006-5
38. Westbroek, P. Electrochemical methods. in *Analytical Electrochemistry in Textiles* (2005). doi:10.1533/9781845690878.1.37
39. Bi, H. & Han, X. Chemical sensors for environmental pollutant determination. in *Chemical, Gas, and Biosensors for Internet of Things and Related Applications* (2019). doi:10.1016/b978-0-12-815409-0.00010-3
40. Scott, K. Electrochemical Principles and Characterization of Bioelectrochemical Systems. in *Microbial Electrochemical and Fuel Cells: Fundamentals and Applications* (2016). doi:10.1016/B978-1-78242-375-1.00002-2
41. Marx, itala M. G. *et al.* Electrochemical sensor-based devices for assessing bioactive compounds in olive oils: a brief review. *Electron. (Basel, Switzerland)* **7**, 387 (2018).
42. Adeloju, S. B. Amperometry. in *Encyclopedia of Analytical Science: Second Edition* (2004). doi:10.1016/B0-12-369397-7/00012-1
43. Gaudin, V. Receptor-based electrochemical biosensors for the detection of contaminants in food products. in *Electrochemical Biosensors* (2019). doi:10.1016/B978-0-12-816491-4.00011-5
44. Shimomura, M., Kuwahara, T., Iizuka, K. & Kinoshita, T. Immobilization of alcohol dehydrogenase on films prepared by the electrochemical copolymerization of pyrrole and 1-(2-carboxyethyl)pyrrole for ethanol sensing. *J. Appl. Polym. Sci.* (2010). doi:10.1002/app.31776

45. Amine, A. & Mohammadi, H. Amperometry. in *Encyclopedia of Analytical Science* (2019). doi:10.1016/B978-0-12-409547-2.14204-0
46. Delahay, P. & Mamantov, G. Voltammetry at Constant Current: Review of Theoretical Principles. *Anal. Chem.* (1955). doi:10.1021/ac60100a001
47. Lockwood, E. H. & Edwards, A. L. An Introduction to Linear Regression and Correlation. *Math. Gaz.* (1985). doi:10.2307/3616472
48. Xu, F., Liu, Y., Xie, S. & Wang, L. Electrochemical preparation of a three dimensional PEDOT-Cu_xO hybrid for enhanced oxidation and sensitive detection of hydrazine. *Anal. Methods* **8**, 316–325 (2016).
49. Luo, J., Sun, J., Huang, J. & Liu, X. Preparation of water-compatible molecular imprinted conductive polyaniline nanoparticles using polymeric micelle as nanoreactor for enhanced paracetamol detection. *Chem. Eng. J.* **283**, 1118–1126 (2016).
50. Yarman, A. & Scheller, F. W. MIP-esterase/Tyrosinase Combinations for Paracetamol and Phenacetin. *Electroanalysis* **28**, 2222–2227 (2016).
51. Filik, H., Aydar, S. & Avan, A. A. Poly(2,2'-(1,4-phenylenedivinylene) Bis-8-hydroxyquinaldine) Modified Glassy Carbon Electrode for the Simultaneous Determination of Paracetamol and p-Aminophenol. *Anal. Lett.* **48**, 2581–2596 (2015).
52. Draper, N. R. & Smith, H. *Applied regression analysis*. **326**, (John Wiley & Sons, 1998).
53. Afshari, M., Dinari, M. & Momeni, M. M. The graphitic carbon nitride/polyaniline/silver nanocomposites as a potential electrocatalyst for hydrazine detection. *J. Electroanal. Chem.* **833**, 9–16 (2019).
54. Miller, J. N. & Miller, J. C. *Statistics and Chemometrics for Analytical Chemistry*. Pearson education Canada (2010).
55. Madhuri, C. *et al.* Electrochemical determination of paracetamol at poly(orange dye) modified carbon paste electrode by using cyclic voltammetry. *J. Chem. Technol. Metall.* **54**, 758–764 (2019).
56. Xie, Z. & Ebinghaus, R. Analytical methods for the determination of emerging organic contaminants in the atmosphere. *Anal. Chim. Acta* **610**, 156–178 (2008).
57. Dirtu, A. C., Van Den Eede, N., Malarvannan, G., Ionas, A. C. & Covaci, A. Analytical

- methods for selected emerging contaminants in human matrices-A review. *Anal. Bioanal. Chem.* **404**, 2555–2581 (2012).
58. Goodson, K. L., Pitt, R., Subramaniam, S. & Clark, S. The effect of increased flows on the treatability of emerging contaminants at a wastewater treatment plant during rain events. in *WEFTEC 2012 - 85th Annual Technical Exhibition and Conference* **11**, 7224–7237 (2012).
59. Arciuli, M., Palazzo, G., Gallone, A. & Mallardi, A. Bioactive paper platform for colorimetric phenols detection. *Sensors Actuators, B Chem.* (2013). doi:10.1016/j.snb.2013.06.042
60. Baek, S., Lee, Y. & Son, Y. Amperometric phenol sensors employing conducting polymer microtubule structure. *Mol. Cryst. Liq. Cryst.* **519**, 69–76 (2010).
61. Prehn, R., Gonzalo-Ruiz, J. & Cortina-Puig, M. Electrochemical detection of polyphenolic compounds in foods and beverages. *Curr. Anal. Chem.* **8**, 472–484 (2012).
62. El-Kosasy, A. M., Riad, S. M., Abd El-Fattah, L. E. & Abd El-Kader Ahmad, S. Novel poly (vinyl chloride) matrix membrane electrodes for the determination of phenolic pollutants in waste water. *Water Res.* **37**, 1769–1775 (2003).
63. Yang, C., Xu, J. & Hu, S. Development of a novel nitrite amperometric sensor based on poly(toluidine blue) film electrode. *J. Solid State Electrochem.* **11**, 514–520 (2007).
64. Qu, J. *et al.* A novel nanofilm sensor based on poly-(alizarin red)/Fe₃O₄ magnetic nanoparticles-multiwalled carbon nanotubes composite material for determination of nitrite. *J. Nanosci. Nanotechnol.* **16**, 2731–2736 (2016).
65. Wang, H., Yang, P.-H., Cai, H.-H. & Cai, J. Constructions of polyaniline nanofiber-based electrochemical sensor for specific detection of nitrite and sensitive monitoring of ascorbic acid scavenging nitrite. *Synth. Met.* **162**, 326–331 (2012).
66. Dong, X., Cui, Y. & Li, T. *Synthesis of carbazole modified glass plate for detecting nitroaromatic compounds.* *Advanced Materials Research* **557–559**, (2012).
67. Wen, Z.-H. & Kang, T.-F. Determination of nitrite using sensors based on nickel phthalocyanine polymer modified electrodes. *Talanta* **62**, 351–355 (2004).
68. Sousa, A. L. *et al.* Amperometric sensor for nitrite based on copper tetrasulphonated

- phthalocyanine immobilized with poly-l-lysine film. *Talanta* **75**, 333–338 (2008).
69. Badea, M. *et al.* New electrochemical sensors for detection of nitrites and nitrates. *J. Electroanal. Chem.* **509**, 66–72 (2001).
70. Toal, S. J. & Trogler, W. C. Polymer sensors for nitroaromatic explosives detection. *J. Mater. Chem.* **16**, 2871–2883 (2006).
71. Ronkainen, N. J., Halsall, H. B. & Heineman, W. R. Electrochemical biosensors. *Chem. Soc. Rev.* (2010). doi:10.1039/b714449k
72. Gu, Y. *et al.* Biomimetic sensor based on copper-poly(cysteine) film for the determination of metronidazole. *Electrochim. Acta* **152**, 108–116 (2015).
73. Xiao, N. *et al.* Carbon paste electrode modified with duplex molecularly imprinted polymer hybrid film for metronidazole detection. *Biosens. Bioelectron.* **81**, 54–60 (2016).
74. Gu, Y. *et al.* Biomimetic sensor based on molecularly imprinted polymer with nitroreductase-like activity for metronidazole detection. *Biosens. Bioelectron.* **77**, 393–399 (2016).
75. Yang, M. *et al.* Sensitive voltammetric detection of metronidazole based on three-dimensional graphene-like carbon architecture/polythionine modified glassy carbon electrode. *J. Electrochem. Soc.* **165**, B530–B535 (2018).
76. Ghadimi, H. *et al.* Electrochemical determination of aspirin and caffeine at MWCNTs-poly-4-vinylpyridine composite modified electrode. *J. Taiwan Inst. Chem. Eng.* **65**, 101–109 (2016).
77. Feng, Q. *et al.* Frontal polymerization and characterization of interpenetrating polymer networks composed of poly(N-isopropylacrylamide) and polyvinylpyrrolidone. *Colloid Polym. Sci.* **296**, 165–172 (2018).
78. Suriyanarayanan, S., Mandal, S., Ramanujam, K. & Nicholls, I. A. Electrochemically synthesized molecularly imprinted polythiophene nanostructures as recognition elements for an aspirin-chemosensor. *Sensors Actuators, B Chem.* **253**, 428–436 (2017).
79. Puangjan, A., Chaiyasith, S., Wichitpanya, S., Daengduang, S. & Puttota, S. Electrochemical sensor based on PANI/MnO₂-

- Sb₂O₃ nanocomposite for selective simultaneous voltammetric determination of ascorbic acid and acetylsalicylic acid. *J. Electroanal. Chem.* **782**, 192–201 (2016).
80. Deiminiat, B., Razavipanah, I., Rounaghi, G. H. & Arbab-Zavar, M. H. A novel electrochemical imprinted sensor for acetylsalicylic acid based on polypyrrole, sol-gel and SiO₂@Au core-shell nanoparticles. *Sensors Actuators, B Chem.* **244**, 785–795 (2017).
81. Wang, P., Gan, T., Zhang, J., Luo, J. & Zhang, S. Polyvinylpyrrolidone-enhanced electrochemical oxidation and detection of acyclovir. *J. Mol. Liq.* **177**, 129–132 (2013).
82. Hamtak, M., Fotouhi, L., Hosseini, M. & Seyed Dorraji, P. Improved Performance for Acyclovir Sensing in the Presence of Deep Eutectic Solvent and Nanostructures and Polymer. *IEEE Sens. J.* **20**, 623–630 (2020).
83. Dorraji, P. S. & Jalali, F. Differential pulse voltammetric determination of nanomolar concentrations of antiviral drug acyclovir at polymer film modified glassy carbon electrode. *Mater. Sci. Eng. C* **61**, 858–864 (2016).
84. Hamtak, M., Fotouhi, L., Hosseini, M. & Dorraji, P. S. Sensitive determination of acyclovir in biological and pharmaceutical samples based on polymeric film decorated with nanomaterials on nanoporous glassy carbon electrode. *J. Electrochem. Soc.* **165**, B632–B637 (2018).
85. Ahmed, A. M. K., Hanoon, I. T. & Ahmed, S. H. Determination of the Ciprofloxacin Hydrochloride Drug in Some Pharmaceuticals using Manufactured Membrane Selective Electrodes. *Syst. Rev. Pharm.* **11**, 622–626 (2020).
86. Hatamluyi, B., Modarres Zahed, F., Es'haghi, Z. & Darroudi, M. Carbon Quantum Dots Co-catalyzed with ZnO Nanoflowers and Poly (CTAB) Nanosensor for Simultaneous Sensitive Detection of Paracetamol and Ciprofloxacin in Biological Samples. *Electroanalysis* **32**, 1818–1827 (2020).
87. Pushpanjali, P. A., Manjunatha, J. G. & Shreenivas, M. T. The Electrochemical Resolution of Ciprofloxacin, Riboflavin and Estriol Using Anionic Surfactant and Polymer-Modified Carbon Paste Electrode. *ChemistrySelect* **4**, 13427–13433 (2019).
88. Chauhan, R., Gill, A. A. S., Nate, Z. & Karpoormath, R. Highly selective

- electrochemical detection of ciprofloxacin using reduced graphene oxide/poly(phenol red) modified glassy carbon electrode. *J. Electroanal. Chem.* **871**, (2020).
89. Zhang, D. *et al.* A label-free colorimetric biosensor for 17 β -estradiol detection using nanoparticles assembled by aptamer and cationic polymer. *Aust. J. Chem.* **69**, 12–19 (2016).
 90. Wang, A. *et al.* A novel electrochemical enzyme biosensor for detection of 17 β -estradiol by mediated electron-transfer system. *Talanta* **192**, 478–485 (2019).
 91. Szychalska, K., Zajac, D. & Cabaj, J. Electrochemical biosensor for detection of 17 β -estradiol using semi-conducting polymer and horseradish peroxidase. *RSC Adv.* **10**, 9079–9087 (2020).
 92. Liu, W. *et al.* Poly(3,6-diamino-9-ethylcarbazole) based molecularly imprinted polymer sensor for ultra-sensitive and selective detection of 17- β -estradiol in biological fluids. *Biosens. Bioelectron.* **104**, 79–86 (2018).
 93. Li, M., Wang, W., Chen, Z., Song, Z. & Luo, X. Electrochemical determination of paracetamol based on Au@graphene core-shell nanoparticles doped conducting polymer PEDOT nanocomposite. *Sensors Actuators, B Chem.* **260**, 778–785 (2018).
 94. Wei, Y., Zeng, Q., Bai, S., Wang, M. & Wang, L. Nanosized Difunctional Photo Responsive Magnetic Imprinting Polymer for Electrochemically Monitored Light-Driven Paracetamol Extraction. *ACS Appl. Mater. Interfaces* **9**, 44114–44123 (2017).
 95. Dai, Y., Li, X., Lu, X. & Kan, X. Voltammetric determination of paracetamol using a glassy carbon electrode modified with Prussian Blue and a molecularly imprinted polymer, and ratiometric read-out of two signals. *Microchim. Acta* **183**, 2771–2778 (2016).
 96. Li, C. *et al.* Electrochemical Determination of Paracetamol at Poly(3-Methylthiophene)/Reduced Graphene Oxide Modified Glassy Carbon Electrode. *Nano* **13**, (2018).
 97. Mohammad Bagher Gholivand & Elahe Ahmadi. Square Wave Anodic Stripping Voltammetric Determination of Paracetamol at Poly Luminol/Functionalized Multi-Walled Carbon Nanotubes Modified Glassy Carbon Electrode. *Russ. J. Electrochem.* **55**, 1151–1161 (2019).

98. Sipa, K., Socha, E., Skrzypek, S. & Krzyczmonik, P. Electrodes modified with composite layers based on poly(3,4-ethylenedioxythiophene) as sensors for paracetamol. *Anal. Sci.* **33**, 287–292 (2017).
99. Bayram, E. & Akyilmaz, E. Development of a new microbial biosensor based on conductive polymer/multiwalled carbon nanotube and its application to paracetamol determination. *Sensors Actuators, B Chem.* **233**, 409–418 (2016).
100. Kuskur, C. M., Kumara Swamy, B. E., Jayadevappa, H. & Ganesh, P. S. Poly (rhodamine B) sensor for norepinephrine and paracetamol: a voltammetric study. *Ionics (Kiel)*. **24**, 3631–3640 (2018).
101. Kuskur, C. M., Kumara Swamy, B. E. & Jayadevappa, H. Poly (naphthol green B) modified carbon paste electrode for the analysis of paracetamol and norepinephrine. *Ionics (Kiel)*. **25**, 1845–1855 (2019).
102. Chitravathi, S. & Munichandraiah, N. Voltammetric determination of paracetamol, tramadol and caffeine using poly(Nile blue) modified glassy carbon electrode. *J. Electroanal. Chem.* **764**, 93–103 (2016).
103. Kaur, B., Prathap, M. U. A. & Srivastava, R. Synthesis of transition-metal exchanged nanocrystalline ZSM-5 and their application in electrochemical oxidation of glucose and methanol. *Chempluschem* (2012). doi:10.1002/cplu.201200236
104. Kaur, B. & Srivastava, R. Simultaneous determination of epinephrine, paracetamol, and folic acid using transition metal ion-exchanged polyaniline-zeolite organic-inorganic hybrid materials. *Sensors Actuators, B Chem.* **211**, 476–488 (2015).
105. Vilela, E. T., Carvalho, R. D. C. S., Yotsumoto Neto, S., Luz, R. D. C. S. & Damos, F. S. Exploiting charge/ions compensating processes in PANI/SPANI/reduced graphene oxide composite for development of a high sensitive H₂O₂ sensor. *J. Electroanal. Chem.* **752**, 75–81 (2015).
106. Luo, M. *et al.* Chemiluminescence biosensor for hydrogen peroxide determination by immobilizing horseradish peroxidase onto PVA-co-PE nanofiber membrane. *Eur. Polym. J.* **91**, 307–314 (2017).
107. Ojani, R., Hamidi, P. & Raoof, J. B. Efficient nonenzymatic hydrogen peroxide sensor in acidic media based on Prussian blue nanoparticles-modified poly(o-

- phenylenediamine)/glassy carbon electrode. *Chinese Chem. Lett.* **27**, 481–486 (2016).
108. Zhou, B., Liang, L. M. & Yao, J. Nanoflakes of an aminoacid-based chiral coordination polymer: Synthesis, optical and electrochemical properties, and application in electrochemical sensing of H₂O₂. *J. Solid State Chem.* **223**, 152–155 (2015).
109. Vilian, A. T. E. *et al.* Immobilization of hemoglobin on functionalized multi-walled carbon nanotubes-poly-l-histidine-zinc oxide nanocomposites toward the detection of bromate and H₂O₂. *Sensors Actuators, B Chem.* **224**, 607–617 (2015).
110. Saidu, F. K., Joseph, A., Varghese, E. V. & Thomas, G. V. Silver nanoparticles-embedded poly(1-naphthylamine) nanospheres for low-cost non-enzymatic electrochemical H₂O₂ sensor. *Polym. Bull.* (2019). doi:10.1007/s00289-019-03053-x
111. Mercante, L. A. *et al.* One-pot preparation of PEDOT:PSS-reduced graphene decorated with Au nanoparticles for enzymatic electrochemical sensing of H₂O₂. *Appl. Surf. Sci.* **407**, 162–170 (2017).
112. Zhang, R. *et al.* A gold electrode modified with a nanoparticulate film composed of a conducting copolymer for ultrasensitive voltammetric sensing of hydrogen peroxide. *Microchim. Acta* **185**, (2018).
113. Chen, C. *et al.* Hydrogen peroxide biosensor based on the immobilization of horseradish peroxidase onto a poly(aniline-co-N-methylthionine) film. *Synth. Met.* **212**, 123–130 (2016).
114. Torres, D. I., Miranda, M. V. & Campo Dall'Orto, V. One-pot preparation of SBP-PANI-PAA-ethylene glycol diglycidyl ether sensor for electrochemical detection of H₂O₂. *Sensors Actuators, B Chem.* **239**, 1016–1025 (2017).
115. Yusoff, F. & Muhamad, N. B. Synthesis and characterization of reduced graphene oxide/PEDOT composite as cathode materials for oxygen reduction reaction. *Mater. Today Proc.* **16**, 2023–2029 (2019).
116. Wang, J., Wang, Y., Cui, M., Xu, S. & Luo, X. Enzymeless voltammetric hydrogen peroxide sensor based on the use of PEDOT doped with Prussian Blue nanoparticles. *Microchim. Acta* **184**, 483–489 (2017).
117. Lete, C. *et al.* Sinusoidal voltage electrodeposition of PEDOT-Prussian blue nanoparticles composite and its application to amperometric sensing of H₂O₂ in human

- blood. *Mater. Sci. Eng. C* **102**, 661–669 (2019).
118. Teker, M. Ş., Karaca, E., Pekmez, N. Ö., Tamer, U. & Pekmez, K. An Enzyme-free H₂O₂ Sensor Based on Poly(2-Aminophenylbenzimidazole)/Gold Nanoparticles Coated Pencil Graphite Electrode. *Electroanalysis* **31**, 75–82 (2019).
 119. Lu, B. *et al.* Cost-effective three dimensional Ag/polymer dyes/graphene-carbon spheres hybrids for high performance nonenzymatic sensor and its application in living cell H₂O₂ detection. *Bioelectrochemistry* **123**, 103–111 (2018).
 120. Cui, H. F., Bai, Y. F., Wu, W. W., He, X. & Luong, J. H. T. Modification with mesoporous platinum and poly(pyrrole-3-carboxylic acid)-based copolymer on boron-doped diamond for nonenzymatic sensing of hydrogen peroxide. *J. Electroanal. Chem.* **766**, 52–59 (2016).
 121. Dai, J. *et al.* Amperometric nitrite sensor based on a glassy carbon electrode modified with multi-walled carbon nanotubes and poly(toluidine blue). *Microchim. Acta* **183**, 1553–1561 (2016).
 122. Hui, N. *et al.* Electrodeposited Conducting Polyaniline Nanowire Arrays Aligned on Carbon Nanotubes Network for High Performance Supercapacitors and Sensors. *Electrochim. Acta* **199**, 234–241 (2016).
 123. Kannan, A., Sivanesan, A., Kalavani, G., Manivel, A. & Sevvil, R. A highly selective and simultaneous determination of ascorbic acid, uric acid and nitrite based on a novel poly-N-acetyl-L-methionine (poly-NALM) thin film. *RSC Adv.* **6**, 96898–96907 (2016).
 124. Dagci, K. & Alanyalioglu, M. Preparation of Free-Standing and Flexible Graphene/Ag Nanoparticles/Poly(pyronin Y) Hybrid Paper Electrode for Amperometric Determination of Nitrite. *ACS Appl. Mater. & Interfaces* **8**, 2713–2722 (2016).
 125. Liu, W. *et al.* Poly(diallyldimethylammonium chloride) functionalized graphene/double-walled carbon nanotube composite for amperometric determination of nitrite. *Electroanalysis* **28**, 484–492 (2016).
 126. Jiao, M., Li, Z., Li, Y., Cui, M. & Luo, X. Poly(3,4-ethylenedioxythiophene) doped with engineered carbon quantum dots for enhanced amperometric detection of nitrite. *Mikrochim. Acta* **185**, 249 (2018).
 127. Wang, G. *et al.* A glassy carbon electrode modified with poly(3,4-

- ethylenedioxythiophene) doped with nano-sized hydroxyapatite for amperometric determination of nitrite. *Microchim. Acta* **184**, 1721–1727 (2017).
128. Ge, Y. *et al.* Electrochemical synthesis of multilayered PEDOT/PEDOT-SH/Au nanocomposites for electrochemical sensing of nitrite. *Microchim. Acta* **187**, (2020).
 129. Zuo, J. *et al.* Sensitive and selective nitrite sensor based on phosphovanadomolybdates H₆[PMo₉V₃O₄₀], poly(3,4-ethylenedioxythiophene) and Au nanoparticles. *Sensors Actuators, B Chem.* **236**, 418–424 (2016).
 130. Shi, S. *et al.* Electrochemically co-deposition of palladium nanoparticles and poly(1, 5-diaminonaphthalene) onto multiwalled carbon nanotubes (MWCNTs) modified electrode and its application for amperometric determination of nitrite. *Int. J. Electrochem. Sci.* **14**, 7983–7994 (2019).
 131. Wang, J. & Hui, N. A nanocomposite consisting of flower-like cobalt nanostructures, graphene oxide and polypyrrole for amperometric sensing of nitrite. *Microchim. Acta* **184**, 2411–2418 (2017).
 132. Abay, I., Denizli, A., Bişkin, E. & Salih, B. Removal and pre-concentration of phenolic species onto β -cyclodextrin modified poly(hydroxyethylmethacrylate-ethyleneglycoldimethacrylate) microbeads. *Chemosphere* **61**, 1263–1272 (2005).
 133. Bi, W., Wang, M., Yang, X. & Row, K. H. Facile synthesis of poly(ionic liquid)-bonded magnetic nanospheres as a high-performance sorbent for the pretreatment and determination of phenolic compounds in water samples. *J. Sep. Sci.* **37**, 1632–1639 (2014).
 134. Bazrafshan, E., Amirian, P., Mahvi, A. H. & Ansari-Moghaddam, A. Application of adsorption process for phenolic compounds removal from aqueous environments: A systematic review. *Glob. Nest J.* **18**, 146–163 (2016).
 135. Goswami, B. & Mahanta, D. Polyaniline coated nickel oxide nanoparticles for the removal of phenolic compounds: Equilibrium, kinetics and thermodynamic studies. *Colloids Surfaces A Physicochem. Eng. Asp.* **582**, (2019).
 136. Khan, N. *et al.* Investigation of CNT/PPy-Modified Carbon Paper Electrodes under Anaerobic and Aerobic Conditions for Phenol Bioremediation in Microbial Fuel Cells. *ACS Omega* **5**, 471–480 (2019).

137. Ozoner, S. K., Yilmaz, F., Celik, A., Keskinler, B. & Erhan, E. A novel poly(glycine methacrylate-co-3-thienylmethyl methacrylate)- polypyrrole-carbon nanotube-horseradish peroxidase composite film electrode for the detection of phenolic compounds. *Curr. Appl. Phys.* **11**, 402–408 (2011).
138. Khor, S. M. *et al.* Poly(hydroxyl ethyl methacrylate) hydrogel matrix for phenol biosensor. in *2003 Asian Conference on Sensors, AsiaSENSE 2003* 207–211 (2003). doi:10.1109/ASENSE.2003.1225020
139. Wei, T., Huang, X., Zeng, Q. & Wang, L. Simultaneous electrochemical determination of nitrophenol isomers with the polyfurfural film modified glassy carbon electrode. *J. Electroanal. Chem.* **743**, 105–111 (2015).
140. Zheng, H., Yan, Z., Wang, M., Chen, J. & Zhang, X. Biosensor based on polyaniline-polyacrylonitrile-graphene hybrid assemblies for the determination of phenolic compounds in water samples. *J. Hazard. Mater.* **378**, (2019).
141. Xiao, Z., Qin, W. & Shi, L. A electrochemical sensor based on poly (sulfosalicylic acid) film modified electrode and application to phenol detection in oilfield wastewater. *Int. J. Smart Home* **10**, 299–308 (2016).
142. Yao, Y. *et al.* Voltammetric determination of catechin using single-walled carbon nanotubes/poly(hydroxymethylated-3,4-ethylenedioxythiophene) composite modified electrode. *Ionics (Kiel)*. **21**, 2927–2936 (2015).
143. Tian, F. *et al.* Synthesis of one-dimensional poly(3,4-ethylenedioxythiophene)-graphene composites for the simultaneous detection of hydroquinone, catechol, resorcinol, and nitrite. *Synth. Met.* **226**, 148–156 (2017).
144. Kuskur, C. M., Kumara Swamy, B. E. & Jayadevappa, H. Poly (naphthol green B) modified carbon paste electrode sensor for catechol and hydroquinone. *J. Electroanal. Chem.* **804**, 99–106 (2017).
145. Aravindan, N., Preethi, S. & Sangaranarayanan, M. V. Non-enzymatic selective determination of catechol using copper microparticles modified polypyrrole coated glassy carbon electrodes. *J. Electrochem. Soc.* **164**, B274–B284 (2017).
146. Guo, Z. *et al.* 1,3,5-Trinitrotoluene detection by a molecularly imprinted polymer sensor based on electropolymerization of a microporous-metal-organic framework. *Sensors*

- Actuators, B Chem.* **207**, 960–966 (2015).
147. Giribabu, K. *et al.* Glassy carbon electrode modified with poly(methyl orange) as an electrochemical platform for the determination of 4-nitrophenol at nanomolar levels. *Curr. Appl. Phys.* **17**, 1114–1119 (2017).
 148. Marinović, S. *et al.* Non-toxic poly(vinyl alcohol)/clay composites as electrode material for detection of 4-chlorophenol and 4-nitrophenol. *J. Electroanal. Chem.* **848**, (2019).
 149. Sobkowiak, M., Rebis, T. & Milczarek, G. Electrocatalytic sensing of polynitroaromatic compounds on multiwalled carbon nanotubes modified with alkoxy-sulfonated derivative of PEDOT. *Mater. Chem. Phys.* **186**, 108–114 (2017).
 150. Sağlam, Ş., Üzer, A., Erçağ, E. & Apak, R. Electrochemical Determination of TNT, DNT, RDX, and HMX with Gold Nanoparticles/Poly(Carbazole-Aniline) Film-Modified Glassy Carbon Sensor Electrodes Imprinted for Molecular Recognition of Nitroaromatics and Nitramines. *Anal. Chem.* **90**, 7364–7370 (2018).
 151. Dechtrirat, D. *et al.* A screen-printed carbon electrode modified with gold nanoparticles, poly(3,4-ethylenedioxythiophene), poly(styrene sulfonate) and a molecular imprint for voltammetric determination of nitrofurantoin. *Microchim. Acta* **185**, (2018).
 152. Sağlam, Ş., Üzer, A., Tekdemir, Y., Erçağ, E. & Apak, R. Electrochemical sensor for nitroaromatic type energetic materials using gold nanoparticles/poly(o-phenylenediamine-aniline) film modified glassy carbon electrode. *Talanta* **139**, 181–188 (2015).
 153. Chen, C., Chen, W., Jiang, J., Qian, L. & Zhang, X. Nitrofurantoin determination in aquaculture water by using poly-alizarin red-modified electrode. *J. Electrochem. Soc.* **166**, H425–H432 (2019).
 154. Yao, C., Sun, H., Fu, H.-F. & Tan, Z.-C. Sensitive simultaneous determination of nitrophenol isomers at poly(p-aminobenzenesulfonic acid) film modified graphite electrode. *Electrochim. Acta* **156**, 163–170 (2015).
 155. Chiu, S.-H., Su, Y.-L., Le, A. V. T. & Cheng, S.-H. Nanocarbon material-supported conducting poly(melamine) nanoparticle-modified screen-printed carbon electrodes for highly sensitive determination of nitrofurantoin drugs by adsorptive stripping voltammetry. *Anal. Bioanal. Chem.* **410**, 6573–6583 (2018).

156. Palma-Cando, A. & Scherf, U. Electrogenerated thin films of microporous polymer networks with remarkably increased electrochemical response to nitroaromatic analytes. *ACS Appl. Mater. Interfaces* **7**, 11127–11133 (2015).
157. Palma-Cando, A., Preis, E. & Scherf, U. Silicon- or Carbon-Cored Multifunctional Carbazolyl Monomers for the Electrochemical Generation of Microporous Polymer Films. *Macromolecules* (2016). doi:10.1021/acs.macromol.6b02025
158. Palma-Cando, A., Brunklaus, G. & Scherf, U. Thiophene-Based Microporous Polymer Networks via Chemical or Electrochemical Oxidative Coupling. *Macromolecules* **48**, 6816–6824 (2015).
159. Palma-Cando, A., Rendón-Enríquez, I., Tausch, M. & Scherf, U. Thin functional polymer films by electropolymerization. *Nanomaterials* (2019). doi:10.3390/nano9081125
160. Calam, T. T. Electrochemical Oxidative Determination and Electrochemical Behavior of 4-Nitrophenol Based on an Au Electrode Modified with Electro-polymerized 3,5-Diamino-1,2,4-triazole Film. *Electroanalysis* **32**, 149–158 (2020).
161. Arulraj, A. D., Vijayan, M. & Vasantha, V. S. Highly selective and sensitive simple sensor based on electrochemically treated nano polypyrrole-sodium dodecyl sulphate film for the detection of para-nitrophenol. *Anal. Chim. Acta* **899**, 66–74 (2015).